ENDOTHELIAL PHENOTYPE DIFFERS BY BOTH SEX AND VESSEL FUNCTION (CONDUIT VS. EXCHANGE)

A Thesis

presented to

the Faculty of the Graduate School

at the University of Missouri-Columbia

In Partial Fulfillment

of the Requirements for the Degree

Master of Sciences

---

by

SCOTT S. KEMP

Dr. Virginia Huxley, Thesis Supervisor

JULY 2017

The undersigned, appointed by the dean of the Graduate School, have examined the thesis entitled

ENDOTHELIAL PHENOTYPE DIFFERS BY BOTH SEX AND VESSEL FUNCTION

(CONDUIT VS. EXCHANGE)

presented by Scott S. Kemp,

a candidate for the degree of Master of Science,

and hereby certify that, in their opinion, it is worthy of acceptance.

Professor Virginia Huxley

Professor Jeff Bryan

Professor Ronald Korthuis

Professor Luis Martinez-Lemus

Professor Alan Parrish

ACKNOWLEDGEMENTS

I would like to dedicate this Master's Thesis to Christine Schramm. I feel it is appropriate that as I write these acknowledgements it is pouring rain outside, for the Earth and heavens beyond seem to weep for the tragic loss of a good person. Suffice to say it was Christine who suggested I apply for the master's program when we met a few years ago. I quite literally would not be here without her. Her knowledge and guidance have made all of my research possible, and her presence will not only be sorely missed by our laboratory, but in all of science; and in all of life. I take solace in her last gift to me, reaffirming that I am on the right career path. Her needless death to sepsis invigorates me with the desire to become a better scientist, so I may contribute to preventing unnecessary deaths of the future.

I too would like to thank Dr. Virginia Huxley for her constant mentorship, and for her patience in the face of my unbridled inquisitive nature. I could not have made it this far without her guidance, and if I did, I know I would be the less for it. I count myself lucky to be one of her trainees, as her commitment to teaching, and science in general is unparalleled. She is truly a credit to her already prestigious family name.

A special thanks to Steve Sieveking for making sure the equipment is always running, and for all of the enjoyable conversations we have had over the last years.

I would like to thank my committee for their belief in me, and for each member going out of their way to make sure I succeed.

I thank my family and friends for shaping me into the person I am today, as very few have been as blessed as I.

Finally, I would like to thank my loving fiancé, Isabella Zaniletti for always supporting me…and giving me help with statistics when I need it ;).

TABLE OF CONTENTS

LIST OF FIGURES

Endothelial Phenotype Differs by Both Sex and Vessel Function (Conduit vs. Exchange)

Scott Kemp, Christine Schramm, Steve Sieveking, Virginia Huxley

Medical Pharmacology and Physiology

University of Missouri, Columbia, MO

While vessel-specific and sex-differences in the functions and responses of continuous endothelium have been observed, the mechanisms responsible for these distinctions remain poorly understood. Our objective is to elucidate the molecular mechanisms, as well as physical differences, responsible for observed vessel-type and sex-differences in basal and activated barrier function of adult rat macro- and microvessels. To this end we focused on endothelial cells (ECs), isolated from age-matched, reproductively mature male and female rats (Sprague Dawley, 67-83 days old) grown under identical conditions to test the hypothesis that ECs will differ in protein expression, when compared by vessel-type or sex. Vascular ECs isolated from aorta (macrovessel) and skeletal muscle (microvessel) from male and female rats, to begin answering our question, and to compare our findings with previously published data. Six markers associated with barrier function were studied: vascular endothelial-cadherin (CD144, VE-CAD), platelet endothelial cell adhesion molecule-1 (PECAM-1, CD31), αvβ3 (Integrin), neural cadherin (NCAD, CDH2), vascular cell adhesion molecule-1 (VCAM-1, CD 106), and intercellular adhesion molecule-1 (ICAM-1, CD 54). In addition, we included the major sex hormone receptors: androgen receptor (AR) and estrogen receptors α and β (ERα and ERβ). Using several techniques, phenotypic differences in cell size, cell growth, cell protein distribution were assessed. Expression of these proteins was conducted in sex-verified (SRY gene expression) macro- and microvascular ECs maintained in identical conditions of culture

(*Passage 4*). Consistent with our hypothesis, marker expression in ECs differed greatly by both sex and vessel type. Furthermore, a recurring trend among our data was a hierarchy of importance as to how predictive cell culture will be to define an EC in the continuous endothelium:

Random Continuous EC < Grouping by Sex < Grouping by Vessel < Grouping by Sex and Vessel Together

Conclusion: When studying functions mediated by vascular endothelium, in vivo or in culture, it is important to use cells from an anatomical/functional location that best describes the question under investigation (or multiple locations if looking systemically), AND both sexes, as both characteristics determine phenotype and/or influence epigenetics.

INTRODUCTION

Preface

Vascular networks of vertebrates are lined ubiquitously with a layer of cells known as the endothelium. Once thought to be an inert "cellophane wrapper,"[1] the endothelium has since been shown to be a highly metabolic organ mediating numerous functions at the blood/tissue interface. The pivotal role of the endothelium is illustrated by the number of chronic disease states associated with altered endothelial function including cardiovascular disease (such as hypertension, heart failure, peripheral vascular disease), kidney failure, multiple autoimmune diseases, diabetes, hypercholesterolemia, obesity, inflammation, and viral infections. Similarly a pivotal role for endothelial dysfunction has been implicated in multiple acute conditions.[1,2,3]

To better understand the complexity of the endothelium, it helps to have some background. With estimates of 60,000 miles of blood vessels in the adult human body covering 4000-7000 m^2 of surface area, made up of 10-60 trillion endothelial cells (ECs), and weighing in around 1kg[2,4,5], it might be expected that ECs display a consistent phenotype. For if there were differences, how would ECs orient themselves throughout the body? Astonishingly, it has been posited that, like snowflakes, no two of the 10-60

trillion ECs in the entire human body are identical. In recent years, the term 'heterogeneity' has gained popularity in describing this phenomenon. Arguments have been made that EC heterogeneity is the hallmark of a healthy vasculature[5]. Even within a tiny vessel, ECs should exhibit heterogeneity. When heterogeneity is lost, endothelial dysfunction ensues.[5,6] If we are to study aspects of the endothelium, be it *in vivo*, *ex vivo*, *in situ*, or *in vitro*, to make generalizations, it is imperative we create touchstones to gauge the relevance of what we are looking at. This thesis will present an argument that EC origin and sex should be cornerstones of experimental designs.

Basic Distinguishable Characteristics of the Endothelium

"Endothelium" is a broad term that includes the cells lining both blood and lymphatic vasculatures. This thesis will focus on the blood vasculature. Even with this distinction, not all blood vasculature is the same. Further, within the blood vasculature the endothelium are broken down into three categories, namely: continuous, fenestrated and discontinuous. Discontinuous endothelium, identifiable by the presence of sinusoidal / fenestrae gaps, are found in organs such as the spleen, bone marrow, and liver that handle transmural movement of large proteins/fat and cell particles. The continuous endothelium can be divided into two categories, non-fenestrated and fenestrated. Non-fenestrated ECs are the 'typical' endothelium, lining the vessels of the skin, lungs, heart, brain, skeletal muscle, and conduit vessels such as the aorta and vena cava. Fenestrated endothelium are specialized ECs located in places like exocrine glands, gastrointestinal mucosa and glomeruli. These cells demonstrate a higher permeability to water and small

solutes, while retaining a similar reflection coefficient for macromolecules relative to continuous EC.[7]

Another distinguishable characteristic of the endothelium reflects the arrangement of the vascular tree. Systemic vessels lined with continuous endothelium can generally be divided into categories from conduit vessels, to feed arteries, to small arteries, arterioles, capillaries, venules, small veins and large veins emptying back into the vena cava for return to the heart. Each part of the vascular tree has a different function. To observe how these differ, a simple cross-sectional area to volume of blood can be analyzed. In an experiment measuring at the average dimensions of mesenteric blood vessels in dogs, it was demonstrated in the categories listed above, 43% of the total cross-sectional area resided in the capillaries, while, by comparison, the main mesenteric artery had a cross-sectional area of 0.13%, and the large mesenteric veins had a cross sectional area of 5.7%. Notably the capillaries, while being the largest contributor of surface area in dog mesentery, contained only 5.7% of the blood volume. This study and similar data illustrate that the majority of vascular surface area lies in the microvasculature, facilitating vascular exchange. In contrast, only 2.5% of the blood volume was contained in the main artery while large veins held 46.7%, highlighting that large veins regulate blood volume and can serve as a reservoir. The muscular arteries have seemingly low blood volume and surface area, but are responsible for much of the regulated resistance between the heart and the exchange vasculature, controlling blood volume, flow distribution, and the pressure gradient. This results in the highest flow rates being seen in the arteries facilitating distribution, and the lowest velocity in the capillaries facilitating exchange.[8]

Differences in wall thickness across the network have also been observed. Capillaries have very thin walls, often lined just by ECs, which minimizes diffusion distance for exchange. On the other hand, muscular arteries and arterioles have a relatively very thick walls, allowing them to withstand relatively high intravascular pressure, and direct blood flow via modulated contraction of vascular smooth muscle cells in their walls.[9] Though we observe functional differences, it is not known whether ECs differ in and of themselves differ between vessel type, or if differences arise from the supporting cells and microenvironment e.g. basal lamina, connective tissue, pericytes, smooth muscle cells, etc..[10] To investigate this question, we will look at differences observed in ECs derived from a conduit and exchange vessel.

Sex

While we want to determine whether it is appropriate to assume phenotypic commonality amongst continuous endothelium, we also want to investigate whether sex differences exist and whether they correlate with sex differences in multiple diseases that are characterized by endothelial dysfunction. Previous work in this laboratory demonstrated numerous sex differences with respect to barrier function in animal models and humans.[11,12,13] While some of these differences might appear small and inconsequential, they are often significant. Interestingly, the data seem to converge on a nexus, being an ability for both sexes to maintain volume homeostasis despite having different basal protein expression. For example, albumin levels differ significantly between men and women until the age of ~50, resting heart rate differs, basal permeability in venules differs, EC phosphodiesterases differ, as do responses to stimuli

such as adenosine.[11,12,13] These observations of EC sex differences are not limited to our laboratory. Indeed, others have observed dimorphic sexual differences in male and female ECs and endothelial progenitor cells (EPCs) as well such as, immune-related genes, responses to shear stress, cell survival, proliferation rates and angiogenic potential .[14,15,16]

A clinical implication of sex differences is observable with respect to pharmaceutical responses. One review highlights several common drug / drug groups exhibiting sex differences. Examples include: aspirin, which has been shown to be less effective at platelet inhibition and heart attack prevention in women, while being less effective in men at preventing strokes. Beta blockers are known to dramatically lower blood pressure and heart rate in exercising women compared to men. Women are more likely to die from taking Digoxin. Women have a greater analgesic response to opioids, are more affected by selective serotonin re-uptake inhibitors, and have reduced affect for tricyclic antidepressants while experiencing an increased response to typical antipsychotics.[17]

We would anticipate observing sex differences with respect to disease prevalence, onset, morbidity and mortality. This has been shown with respect to heart disease: Men typically develop heart disease 7-10 years earlier.[18] Women have a better prognosis for cerebrovascular events, including morbidity and mortality, than age-matched men[19]; a process proposed to result from differences in sex hormones acting on the endothelium--testosterone increasing myogenic tone, estrogen reducing myogenic tone. [20] Almost 80% of people with autoimmune disease are female.[21] In type 2 diabetes, women have a

dramatic increase in risk of myocardial infarction when compared with age matched men with type 2 diabetes.[22]

It is our hypothesis that the endothelium is strongly tied to all of these events, and that sex, influenced by genomics, sex hormones, or epigenetics will result in sex-specific ECs phenotypes.

Permeability

The microvasculature can be divided into three components: 1. Arterioles, the major regulators of blood volume delivered to and pressure within the capillaries, 2. Capillaries, the smallest vessels in the body and a major site of fluid and solute exchange; 3. Venules, the major site of fluid movement and immune response. Within these segments, flux of materials between the vascular and tissue compartments is influenced by EC architecture as well as oncotic and hydrostatic pressure gradients, EC glycocalyx composition, cell depth, inflammation, regulators of transcellular and paracellular pathway structure, extracellular matrix (ECM) and junctional proteins (tight, adherens, gap), and integrins, to name a few.[23,24,25,26] Given that the research focus of this laboratory has been regulation of vascular permeability and given that the laboratory has observed sex differences with respect to both basal permeability and the permeability responses to a variety of stimuli, we decided to focus on the role of genomic sex as it applies to endothelial phenotype under basal conditions.

Objective

Because of the complexity of these subjects, our goal was to create an understanding for the basis for sex-based differences by focusing on major components

(proteins) in ECs. For simplicity's sake, we chose a macrovessel source of ECs (the aorta) and tissue-specific source of microvessel ECs (skeletal muscle). These were not chosen at random, but for specific reasons. We wanted to select vessels with the most common type of EC, e.g. not fenestrated, or overly specialized (e.g. ECs comprising the blood-brain-barrier). The aorta was chosen because it is a large vessel from which EC are relatively easy to harvest and about which there is an extensive literature. While the sex of the animals from which the aortic EC were derived is not often provided in published reports, most animal studies are conducted on males. Given that the responses of macrovessels and microvessels differ significantly, and given the fact that conduit and microvessels play different roles in the functioning of an intact vasculature, we then chose EC isolated from skeletal muscle as aggregate skeletal muscle is the largest organ of the body. Therefore, the endothelium lining this vasculature represents the largest site for microvascular exchange. In addition we chose skeletal muscle of the abdominal free wall because the majority of *in vivo* functional microvascular studies in skeletal muscle are conducted on cremaster muscle (male) which is derived from the abdominal free wall. In this way we facilitate comparison between the data in the literature on males with what we would obtain in this study.[27] In addition, research on sex differences with respect to intact microvascular permeability has been reported on arterioles and venules isolated from the abdominal free wall.

Our goal was to systematically investigate the relative presence of nine proteins, amongst the four tissue types: male aorta (MA), female aorta (FA), male skeletal muscle (MS) and female skeletal muscle (FS). The nine proteins included: three sex hormone

receptors, two junctional proteins, two EC-white blood cell (WBC) proteins, and two EC-Extracellular matrix (ECM) proteins, described in more detail below.

Sex Hormone Receptors

Because we are looking at sex differences, it was logical to determine which sex hormone receptors were expressed by our endothelial cells. Our three targets were the predominant receptors for the sex steroids: androgen receptor (AR), estrogen receptor-α (ERα) and estrogen receptor-β (ERβ).

The estrogen receptor (ER) family is incredibly complex. In addition to the two main receptors, ERα and ERβ, there are several isoforms with the ability to hetero- or homodimerize in a multitude of ways.[28,29] However, we summarize some general characteristics that have been observed in ERs of ECs. ERα and ERβ have been shown to have some redundant effects. In one study, it was found that both are capable of reducing inflammatory cytokine actions mediated by ECs, as well as EC-mediated ECM stabilization (potentially illuminating a reason why males have a higher incidence of aortic aneurisms than females) and by inhibiting EC production of endothelin-1 (ET-1).[30] All of these factors are believed to be vascular protective. However, the 2 receptors are known to differ in significant ways. 17β-estradiol (E2), for example, will induce vascular re-endothelialization via ERα exclusively. It was required that not only endothelial cells express ERα, but that ERα also be expressed by endothelial progenitor cells. [31] ERβ has been shown to be down-regulated when cells are exposed to lipopolysaccharide (LPS), but ERβ mRNA was increased 8-fold after four days of stimulation with E2, possibly

showing down regulation of ERβ during inflammation, and a rescue effect by estrogen. [32] In general, estrogens appear to enhance nitric oxide production in ECs, promote angiogenesis and wound healing, have pro-inflammatory effects (possibly in conflict with what was found above), and at the same time exert anti-atherogenic effects.[33] It is possible that the conflicting results arise as a result of interactions with the dimerized receptors or isoforms of the receptors.

Sex differences have been observed with respect to estrogen's interaction with ECs. For example, skeletal muscle arterioles from females rats are able relax to a greater extent than those from males due to endothelium-dependent NO generation, which was shown to be mediated by the greater amount of endogenous estrogen present in the females.[34]

Encoding for the AR is located on the X-chromosome, so it will be present on both males and females.[35] Data regarding the effect of AR in the vasculature are seemingly contradictory. A recent literature review notes a poor understanding of AR's function, as some investigators have found AR to be vascular-protective while others have reported AR to be harmful to the vasculature.[36] Still others have found that different androgenic hormones have disparate effects on both smooth muscle and ECs, both dependent and independent of AR.[37] One group even found androgens to up-regulate angiogenesis in male ECs, but not in female ECs, via AR.[38]

From a more clinical standpoint, male vasculature in erectile dysfunction (ED) provides an interesting insight to the interactions of ECs and androgenic hormones. It is posited that due to the increased density of ECs in the cavernosal artery, along with the arteries smaller than normal diameter, ED is an early indicator of systemic endothelial

dysfunction, often coinciding with low testosterone. [39] Indeed, low testosterone has been demonstrated to damage ECs, observable by electron microscopy.[40] This may give credence to the protective effects of AR.

Untangling the precise roles of each of these sex hormone receptors will take time given the complexity of each of these systems. In this study, we will take the first step of determining whether differences in sex hormone receptor expression exist at the macro- and microvascular levels.

Junctional Proteins

In ECs, 'junctional proteins' refers to several groups of proteins found in the paracellular junction. These include adherens junctions (AJ), tight junctions (TJ), and gap junctions (GJ)[23]. GJ are small pores facilitating the transmission of small molecules and ions between ECs facilitating cell-cell communication, TJ are barriers and regulators of permeability, and AJ are regulators of permeability, paracellular leukocyte trafficking and cell-cell contact inhibition.[23,41] Our goal was to focus on two proteins: vascular endothelial cadherin (VE-CAD, CD144), and platelet endothelial cell adhesion molecule (PECAM-1, CD31), present in AJ.

Cadherins are named for their calcium-dependent adhesion. The two cadherins expressed in ECs are VE-CAD and neural cadherin (NCAD, CDH2). Both are examples of classic cadherins[42] and possess lateral homodimers that interact with homodimers extended from other cells. These proteins extend out of the EC and connect internally to the actin cytoskeleton via α-catenin, β-catenin, plakoglobin, vinculin and proteins

facilitating inside-out and outside-in signalling.[43] VE-CAD is a vital protein (literally); knocking out VE-CAD results in embryonic lethality due to defects in blood vessel formation.[44] Additionally, VE-CAD is tied to multiple proteins including VE-PTP (receptor-type tyrosine-protein phosphatase beta), PECAM-1and VEGFR2 (vascular endothelial cell growth factor 2) that mediate multiple EC functions in addition to several intracellular signaling pathways, cell-cell adhesion, actin cytoskeleton remodeling, cell-cell growth inhibition and barrier function.[42]

PECAM-1 is another protein that occurs in the AJ. Although we have placed it with the junctional proteins, an equally good argument could be made to place it in the EC-white blood cell (WBC) category. In addition to being found on most leucocytes and platelets, PECAM-1 is also located on EC. To better understand the role of PECAM-1, many knockout animals have been studied. In PECAM-1 knockout animals, neutrophils became much less polarized and were unable to direct themselves towards a chemoattractant.[45] PECAM-1-deficient mice have also been shown to have smaller areas of atherosclerotic lesions, and lower levels of vascular cell adhesion molecule (VCAM-1), and intercellular adhesion molecule 1 (ICAM-1) expression.[46] The basal permeability of PECAM-1-deficient mice is lower than wild type mice (male); and were demonstrated to elicit an exaggerated permeability response when stimulated with a vasoactive substance or inflammatory instigators.[47] PECAM-1 has been implicated in cell-cell adhesion, and angiogenesis.[48] PECAM-1 is known to signal both inside-out and outside-in (depending on the environment, shear stress), to be involved in diapedesis, and form complexes with VE-CAD and VEGFR2.[46]

Endothelial Cell--White Blood Cell (EC-WBC) Interactions

Leukocytes attachment to the endothelium is a hallmark of the inflammatory response in the vasculature. In inflammation, leukocytes on ECs will go through a series of events including capturing, rolling, firm adhesion, crawling, and transmigration. These events are mediated primarily by selectins and cell adhesion molecules (CAMs).[49] We chose two proteins in the immunoglobulin supergene family: ICAM-1 and VCAM-1 given their importance in EC function and changes with dysfunction.

ICAM-1 is upregulated in animal models with atherosclerosis, as well as many other immune responses.[7] In addition to being an attachment molecule for leukocytes, ICAM-1 induces signaling that rearranges the actin-cytoskeleton, aiding in leukocyte transmigration through the EC barrier.[50] ICAM-1 can be activated and upregulated by TNF-α [23]. Interestingly, ICAM-1 receptor density has been observed to play a crucial role for leukocytes to attach to the endothelium, i.e., it is not the number of receptors that a cell possesses, but rather the density of receptors being exposed to the leukocytes.[51] Studies have shown ICAM-1 mediates permeability of ECs, possibly through more than one signaling pathway. [52,53]

While the above states that ICAM-1 is upregulated in atherosclerosis, it has been argued that VCAM-1 is the major regulator of the pathogenesis of early atherosclerosis.[54] Additionally, when VCAM-1 becomes activated, low levels of H_2O_2 are generated which in turn, activates matrix metalloproteinases (MMPs). The MMPs are thought to then be distributed into the blood resulting in remote organ injury in addition to breaking down the barrier around the local EC and exposing matricryptic sites on adhesion molecules and ECM.[55]

While ICAM-1 and VCAM-1 are expressed on the surface of ECs, it is important to remember that ICAM-1 and VCAM-1 can become soluble. Soluble ICAM-1 (sICAM-1) and VCAM-1 (sVCAM-1) are known to be upregulated in certain conditions including vasculitis, heart transplant, and pulmonary fibrosis.[56] However, different vascular beds may elicit different responses. A group found that human umbilical vein endothelial cells (HUVEC, marcrovessel) release sVCAM-1 when stimulated with an endotoxin, whereas sICAM-1 was preferentially released from human dermal microvascular EC (HMEC-1; microvessel) when stimulated with endotoxin. This outcome implies a heterogeneity in ECs from different vascular beds.[57]

Endothelial Cell—Extracellular Matrix (EC-ECM)

The EC barrier *in vivo* includes not only the ECs but also the matrix on which it sits and the cells in the parenchyma of a vessel, which contact and communicate with the EC. At the level of the capillary and venules the primary cell of interest associated with the EC is the pericyte, while in the arterioles it is vascular smooth muscle. Of the remaining proteins we targeted in this study NCAD could have fallen into several categories. One of the reasons we chose NCAD is the literature suggesting that it is necessary for EC-pericyte interactions. When NCAD is blocked, irregularities are seen with respect to blood vessel maturation and pericyte organization.[58,59,60] For this reason we decided to placed NCAD in the category of EC-ECM. The role of EC NCAD remains poorly understood with respect to EC health or disease, despite intensive investigation. What is known is that NCAD is expressed across the entire cell, in contrast VE-CAD which is located primarily in the cell junctions. Knocking out NCAD results in

embryonic lethality, implying that VE-CAD and NCAD are not redundant. Further, they appear to be interlinked as loss of NCAD results in a reduction in EC VE-CAD.[61]

Integrins are proteins that often interact with the ECM, as well as other cells to maintain cell integrity, allow for motility, signal transduction, help with new vessel formation, and cell polarization .[62,63,64] Of the integrins associated with continuous EC we chose $\alpha_v\beta_3$ as a widely studied integrin known to play a role in angiogenesis, tumor formation, repair of vascular damage, and association with arg-gly-asp (RGD) peptides.[65,66] While other integrins may have provided more information about a steady state $\alpha_v\beta_3$ facilitates study of EC phenotype in a dynamic state, perhaps providing insight as to how the cells are growing or moving in males vs. female, and the environment of macro- vs. microvessels.

HYPOTHESIS

The primary hypothesis of this thesis is that the expression of selected proteins associated with endothelial phenotype will vary by sex or origin of EC along the vascular tree, when exposed to a uniform set of conditions (including but not limited to cell media, growth time, temperature, humidity, substrates).

METHODS AND MATERIALS

*- For solutions see "Appendix 2".

Animals

Endothelial cells were harvested from age-matched (67-83 day-old), sexually mature, male (275-375 g) and female (200-300 g) Sprague Dawley® rats (Envigo, Huntingdon, Cambridgeshire, UK)). At sexual maturity there is already a difference in body weight that continues to widen with time as the males continue to grow while the female weight plateaus.

All animal protocols were approved by the Institutional Animal Care and Use Committee at the University of Missouri-Columbia and were conducted in accordance with the National Institutes of Health's "Guide for the Care and Human Use of Laboratory Animals." The rats were euthanized with an overdose of the anesthetic Inactin® hydrate C-IIIN (Thiobutabarbital, Sigma-Aldrich, St. Louis, MO) followed by exsanguination.

General Tissue Preparation

On the day of surgery the rats were anesthetized with an intraperitoneal injection of *Inactin® at 130 mg/kg. Once the rats were fully sedated (non-responsive to toe squeeze), fur and skin were removed from the anterior abdominal wall. Tissue isolation was performed in duplicate, e.g. two males or two females allowing for a larger harvest

of endothelial cells. The two populations of isolated cells were mixed to randomize the populations of cells.

Isolation of Skeletal Muscle Endothelial Cells

To obtain skeletal muscle ECs, the abdominal free wall was excised using sterile techniques and placed in solution of *TBC#1. Separating the abdominal free wall into its internal and external layers exposed a rich field of microvascular trees. Excess tissue (fascia, fat (which there was very little) and myocytes) was removed under dissecting microscope. Care was taken to preserve microvascular network. As the microvasculature was cleaned, it was placed in a sterile petri dish with a solution of *TCB#2. Once all microvasculature had been isolated it was moved into a new, clean petri dish with as little solution as possible, minced with scissors, placed into a 5 mL tube with 4 ml of *digestive enzyme cocktail and then incubated for 1 hour at 37°C. Rat skeletal muscle endothelial cells isolation followed the approach of Wang et al., 2010[11], with the major difference being, cells were now isolated with PECAM-1 coated with MagnaBind™ (Thermo Scientific, Waltham, MA, USA) instead of Dynabeads™ (Dynal, Brown Deer, WI) coated with *Griffonia Simplicifolia* lectin. Additionally, composition of *cell media changed slightly (e.g. percent of FBS in cell media).

Following an hour of digestion, the material was strained first through a 100 μm cell strainer into a fresh tube and subsequently through a 40 μm cell strainer prior to 8 minutes centrifugation at 250x g. Supernatant was removed from the tube and placed into a fresh tube, which was then centrifuged for 5 minutes at 600x g. Next the supernatant was carefully removed, leaving the deposited pellet on the bottom. The cell pellet was then re-suspended with 1 ml of *TCB#3 and transferred to a fresh tube prior to

addition of 30 ml of TCB#3. Tube was centrifuged for 5 more minutes at 600x g and supernatant was discarded. The pellet was re-suspended in 9.5 ml TCB#3 and transferred to a round bottom tube, where 0.5 ml of magnetic *CD31-coated MagnaBind™ (Thermo Scientific, Waltham, MA, USA) were then added to the cell suspension and incubated at room temperature for 30 minutes on a rocking shaker, set to a slow speed. Next the tube was placed in a magnetic holder for ~3 minutes, after which all fluid was removed slowly leaving the cells and beads attached to the magnet. An additional 5 ml of TCB#3 was added, and the tube was mixed prior to a second placement in the magnetic holder. This entire process was repeated for a third time. After the final supernatant was removed, 5 ml of cell media was added, this solution containing cells was mixed, and finally put on a gelatin-coated *T25 flask. The next morning cell media was removed and fresh cell media was added to flask.

Isolation of Aortic Endothelial Cells

The aorta was isolated from the same rats as the skeletal muscle (see above) Once the abdominal free wall was removed, using small scissors, the ribcage was opened, exposing the heart and proximal aorta. Spleen, lungs, and liver were removed to facilitate access to the aorta.

With rat in a supine position, and starting at the lower abdominal level of the aorta, scissors were pressed flat against the spine beneath the vessel, and a cut was made parallel to the spine moving upward towards the chest. The aorta was removed from the fascia using tweezers to gently lift the vessel as it was freed while cutting the fascia with

the other hand. This was done slowly to ensure absence of nicks or cuts to the vessel. The end cut was made to the proximal aorta near the exit of the heart. This gave the longest section of aorta possible.

Once removed, aorta was placed on a Silgard™ (Dow Corning)-coated dish filled with TCB#1. The dish was then placed underneath the microscope, all excess tissue (fat, fascia, etc.) was removed from the aorta using two pairs of forceps, one to keep the tissue in place, the other to remove tissue. After the aorta was cleaned, dissecting scissors were used to cut the aorta in half, lengthwise, allowing the interior of the vessel to be exposed. Any coagulated blood was removed prior to placing the aorta into digestive enzyme cocktail with the endothelium facing upward (~3 mL of digestive enzyme cocktail was sufficient for our experiment). Minutin™ insect pins (100 µm, Carolina Biological, NC) were placed in the aorta to hold it flat, exposing the entirety of the aortic endothelium to the digestive enzyme cocktail. A cover for the dish was then placed over the digesting tissue to limit evaporation of enzyme during 30 minutes in the incubator (37°C, 5% CO_2 95% N_2). Following incubation, while holding onto one side aorta with tweezers, a spatula was used to gently remove the endothelium, scraping away from tweezers. This process was repeated 5 times with the removed material being shaken into a 50 ml tube containing 15 ml of solution TCB#3. This was then repeated five more times, for 25 total scrapes. Once this was completed, cells in TCB#3 solution were centrifuged for 15 minutes at 600x g and the supernatant carefully removed, leaving a pellet at bottom of tube. 5 ml of cell media was placed on top of pellet and gently the pellet was re-suspend. This solution was transferred into a gelatin-coated T25 flask.

Endothelial Cell Isolation and Culture (Aorta and Skeletal Muscle)

Once the initial harvest of aortic and skeletal muscle endothelial cells, in their respective T25 flasks, reached 50% confluence, cell media was removed. Cells were then washed with 5 ml of *DPBS, then 1 ml of *trypsin was added for 20 seconds, which was removed after the 20 seconds. Cells were incubated at 37°C for 1-2 minutes (until cells could be seen with the naked-eye to be detaching). Then 5 ml of TCB#3 was added. Cells and TCB#3 were moved to a round bottom tube, and 250 µl of CD31 magnetic beads were added. Process was repeated as listed above for the skeletal muscle microvascular cells.

When the EC reached 90% confluence, the cell media was once again removed. The T25 plate was washed with DPBS, and 1 ml of trypsin was added. Trypsin was left on for 20 seconds and removed, cells were incubated 1-2 minutes at 37 °C (until cells could be seen detaching) then 5 ml of cell media was added. Cells were then transferred to 2 gelatin-coated T25 flasks. Once 90% confluence had been reached the process was repeated, and these cells were split into 2 gelatin-coated *T75s.

When cells reached 90% confluence on *passage 4*, cell media was removed from plates and plates were washed with 10 ml of DPBS. Cells were trypsinized in the same conditions as above, except 2 ml of trypsin were added per plate, due to the larger plate size. Once cells were detaching 5 ml of cell media were added per plate to suspend and move trypsinized cells.

At this point the EC were counted in the Cellometer® Auto T4 (Nexcelom Bioscience, Lawrence, MA, USA) once dyed with Trypan Blue (Modified) 0.4% w/v

Solution 1N Phosphate Buffered in saline (MP Biomedicals, Inc, Santa Ana, CA, USA). The EC were next centrifuged for 5 minutes at 200x g and supernatant was carefully removed. Finally the cells were re-suspended in *freezing media at a cell concentration of $2x10^5$/ml. Aliquots of 1 ml/vial were labeled and frozen at -70°C. EC verification was achieved by staining for CD31, VE-cadherin, vWF, uptake of acLDL, and capillary like tube formation on Matrigel™, as described in Wang et al., 2010[11]. Passage number after freezing would be denoted by a number after the decimal e.g. cells used on passage two after being unfrozen would be denoted: *passage 4.2*.

Endothelial Cell Culture for Experiments

All EC were grown on T25/T75 gelatin-coated plates to a maximum of passage 4.4. EC were grown in cohorts of four: male aorta, female aorta, male SKM, female SKM, with all conditions remaining identical (taken out of the freezer at the same time, used same cell media, same gelatin, in the same incubator, passaged at the same time. Due to growth differences, some cells were discarded when passaging. This was done in an attempt to standardize the cell numbers, and allow for confluence (or close) to be achieved at the same time.

Immunocytochemistry

Cells were seeded in black, clear-bottom 96-well plates, $1x10^4$ cells/well and grown to confluence (24-48 hr.). The cells were grown in cell media for 48 hours on glass coverslips that had previously been coated with gelatin for 30 minutes.

After cells had grown to confluence, they were fixed for 15 minutes with 4% v/v paraformaldehyde solution in DPBS. Next, cells were washed 3x with 0.1% v/v Triton X-100 in DPBS, then the cells were blocked for 1 hour with 6% w/v normal goat serum and 0.6% v/v Triton X-100 in DPBS. For primary antibodies: dilutions of 1:100 or 1:200 in DPBS with 0.2% w/v bovine serum albumin, globulin-free, and 0.3% v/v Triton X-100, and were refrigerated overnight. The next morning, the preparations were washed 3 times with wash buffer, then secondary antibody was applied at dilution in DPBS with 0.2% w/v Bovine serum albumin, globulin free at room temperature (1 hour).

β-Tubulin was used as a reference to normalize the expression of the proteins of interest, as well as for cell surface area quantification, using Leica TCP SP8 MP microscope in the Molecular Cytology Core at University of Missouri-Columbia and ImageJ (NIH) software[67]. All measurements were made before *passage 4.2*. Nuclei were stained with NucBlue® Fixed cell stain (Life Technologies Corporation, Eugene, OR) to perform a cell count.

Cell size

Cell size was determined by counting using the Cellometer™ Auto T4 imaging cytometer (Nexcelom Bioscience). Cell size was measured by the diameter (μm) of the freely suspended cells in the counting chamber, as determined by image analysis by the Cellometer Auto software. All measurements were made at *passage 4.2*.

Cell Growth Rates

The CyQuant® Cell Proliferation Assay Kit (Molecular Probes®, Life Technologies) was used to evaluate cell growth. On day 0, cells were seeded in triplicate in 96-well plates at 0.8 – 1.0 x 10^4 cells per well in 150µl CM per well, with all cell types being studied. Empty wells were filled with DPBS, and the plates were incubated at 37°C. After the cells attached on day 0, and each subsequent day, the medium was drained from a plate, and the plate was wrapped in plastic and stored at -70°C. When all the plates had been collected and stored, the assay was performed according to instructions, including a calibration curve prepared from an aliquot of cells of known concentration prepared on Day 0.

Flow Cytometry

Briefly, once cells had grown to confluence on *passage 4.4,* 2 mL of Trypsin was added to each T75 plate. Plates were then incubated at 37°C for ~two minutes (until cells detached) then 3 mL of cell media was added to each plate. Cells were counted by Cellometer®, centrifuged at 250x g, the supernatant removed, and the cells were diluted to ~ (1 to 5) x10^6 cells in 2% v/v FBS in PBS. Then 100 µl of cells in 2% v/v FBS was added to individual plastic tubes. Tubes were divided into controls and proteins of interest. Cells were mixed with 100 µl of 0.02% v/v paraformaldehyde in PBS and incubated for10 minutes at room temperature. Next, 300 µl of 0.1% v/v Triton in PBS was added, incubated at room temperature for 10 minutes before addition of 2 ml of PBS to each tube. All tubes were then centrifuged at 250x g, and supernatant was carefully removed. Next, primary antibody was diluted into 100 µl 2% FBS in PBS. Three controls were used for each vessel/sex type: a negative control with no antibody, a

negative control with secondary antibody to mouse and a negative control with secondary antibody to rabbit. Cells were incubated for 30-60 minutes at 4 °C in the dark. After incubation, 2 ml of PBS was added, and cells were centrifuged at 1500 rpm for 5 minutes, thereafter supernatant was carefully removed. Next, secondary antibody was added to appropriate cells. All primary antibodies, except that for $\alpha_v\beta_3$, used a secondary antibody that was either *anti-mouse or anti-rabbit. Secondary antibody was diluted in 100 µl of 2% v/v FBS in PBS per tube. Cells were incubated for 30-60 minutes at 4 °C in the dark. After incubation, 2 ml of PBS was added to each tube. Tubes were centrifuged for 5 minutes at 250x g, and then the supernatant was carefully removed. 500 µl of 2% v/v FBS in PBS was added to each tube, tubes were then stored in ice, in the dark. Using BD LSRFortessa™ X-20 (BD Biosciences | Becton, Dickinson and Company (BD), Franklin Lakes, NJ, USA) in the Cell Immunology Core at University of Missouri. All flow cytometry was performed within a couple of hours after being put on ice.

Flow Cytometry Analysis

Flow cytometry was analyzed using FlowJo™ software (FlowJo LLC, Ashland, OR, USA). Minimal gating was performed to eliminate signal from potential debris, but not influence the data. Gating was applied uniformly to negative controls and target proteins (Figure 1A). Figure 1A is a snapshot of gating for male aorta (MA) of $\alpha_v\beta_3$ protein expression. This image compares forward scatter (FSC-A) on the x-axis with side scatter (SSC-A) on the y-axis. FSC-A is an estimation of the particle size, while SSC-A is particle complexity often described as granularity[68]. Figure 1B is the gated data from Figure 1A, but now Alexa Fluor® 647 is on the x-axis (an arbitrary unit, in which

fluorescence intensity is logarithmically graphed), and SSC-A is once again on the y-axis. This shows the relative intensity of each cell (each point). Experiments were all performed in duplicate (Figure 1C). Male and female protein expression were then compared to a negative control expression. To do this, median fluorescent intensity (MFI) of the negative control was subtracted from MFI of experimental subject (Highlighted values in figure 1C). Medians were used as these graphs are logarithmic, i.e. the population is not normally distributed, making the median a better representation of the population. In this example, protein expression of $\alpha_v\beta_3$ was investigated. This was then compared to the opposite sex and to other vessel location. An average was then assessed using the difference between duplicate experiments. For comparison of differences between overall sexes or vessel origin of target proteins, experiment was performed in the same way, except now combining two previously distinct categories (e.g. male and female for sex differences, male aorta and female aorta for vessel origin differences).

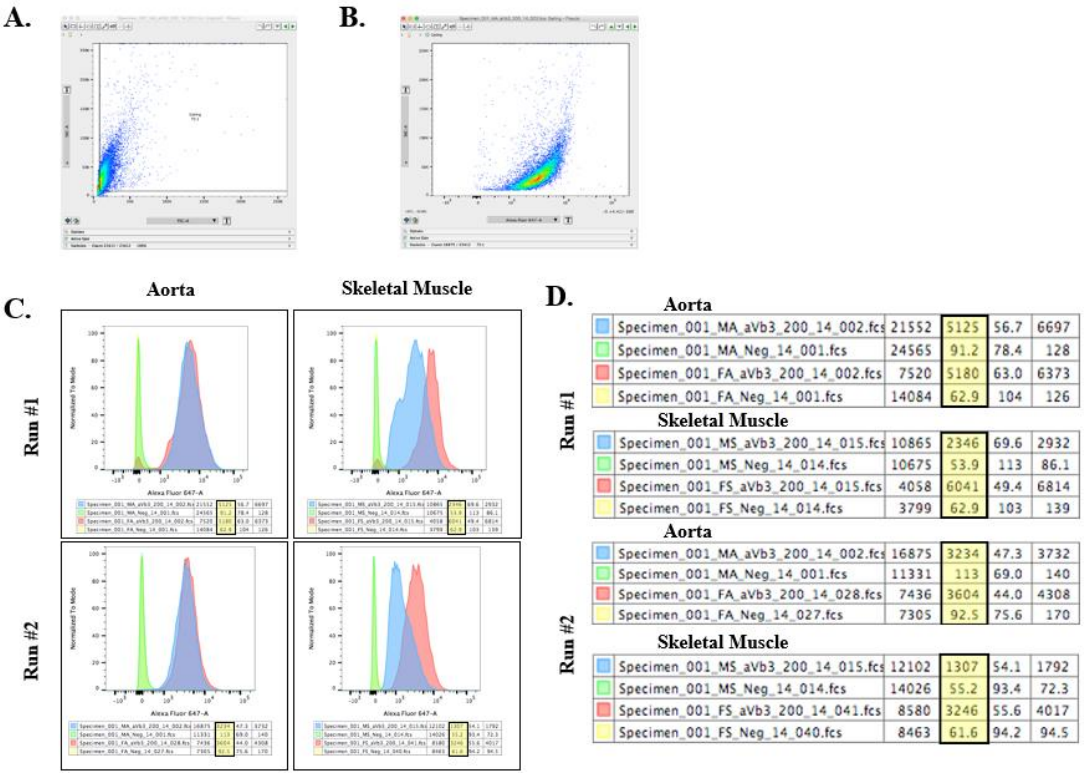

Figure 1: Flow cytometry gating and measurements. Flow cytometry was used to analyze protein expression. $\alpha_v\beta_3$ for male aorta (MA) scatter plot was used as an example of gating (shown above). Shown is a heat map (red = higher density of cells, blue = lower density of cells) (A). After gating, protein expression was measured using relative fluorescence of secondary antibody Alexa Fluor® 647 (B). All measurements for a given protein were done in tandem, i.e. Run #1 had $\alpha_v\beta_3$ measurements for male aorta (MA), MA negative control, female aorta (FA), FA negative control, male skeletal muscle (MS), MS negative control, female skeletal muscle (FS) and FS negative control, all performed under same conditions on same day. Run#2 was performed in the same manner. Highlighted in yellow are the median fluorescent intensity (MFI) values. Due to the logarithmic scale of this graph, these values were not normally distributed, so median instead of means were used to analyze differences in populations (C). Enlargement of numbers presented in Figure C (D).

Antibodies

The cultured EC were incubated for 30 minutes with primary antibodies: to Androgen Receptor (AR, D6F11, Rabbit mAB, 1:200, Cell Signaling Technology), CD31 (PECAM-1, TLD-3A12, Mouse mAB, 1:10 ThermoFisher Scientific), ICAM-1 (CD54, Mouse mAB, 1:100, ThermoFisher Scientific), NCAM (CD56, 3H15L12, Rabbit mAB, 1:100, ThermoFisher Scientific), Estrogen Receptor alpha (ERα, E115, Rabbit mAB, 1:200, Abcam), Estrogen Receptor beta (ERβ, rabbit pAB, 1:200, Abcam), Alpha V + Beta 3 (αvβ3, Rabbit pAB, conjugated primary AB with ALEXA FLUOR® 647, 1:200, Bioss), NCAD (CDH2, 5D5, Mouse mAB, 1:100, ThermoFisher Scientific), VCAM-1 (E1E8X, Rabbit mAB, 1:100, Cell Signaling Technology) and VE-cadherin (3D5C7, CD144, Mouse mAB, 1:50, ThermoFisher Scientific). All used a secondary antibody except for αvβ3. Secondary antibodies were: Alexa Fluor® 647 –conjugated AffiniPure Goat Anti-Rabbit IgG (H+L) (1:200, Jackson Immuno Research Labortories, Inc.) and Cy™5-Conjugated AffiniPure Goat Anti-Mouse IgG. $F_{C\gamma}$ Fragment Specific (minimal cross-reaction to Human, Bovine, and Horse Serum Proteins (1:100, Jackson Immuno Research Laboratories, Inc.). All dilutions were performed with 3% v/v FBS in PBS.

Statistics

Statistical tests were performed using Software SAS 9.4 (Cary, NC) to analyze normality using Anderson-Darling (P<.005), and non-parametric Wilcoxon Rank Sum Test for independent sample and non-normal distributions[69], as well as Individual growth models for exploring longitudinal data over time. The structure of the variance-covariance matrix of the repeated measurements was also analyzed and entered in the model[70]. Statistical significance was set at $P<0.05$.

RESULTS

Given that our hypothesis was that expression of selected proteins associated with EC phenotype will not vary by sex or vessel origin, when exposed to a uniform set of conditions (cell media, growth time, temperature, humidity, substrate, etc.), we needed to first confirm that we had isolated and grown up ECs and not another cell type. To do this, we used a number of well-known EC protein markers that play a role in a diverse array of EC functions, including barrier function, cell adhesion, signaling and sex, growth rates *in vitro*, as well as several morphological characteristics and expression of sex hormones.

Immunocytochemistry (ICC) was used to identify the presence of several proteins (Figure 2A-E). Well-known EC biomarkers are PECAM-1 and VE-cadherin. PECAM-1 (CD31) binding was the basis for the selection method used to isolate our cells. It therefore stands to reason that we should see a presence of PECAM-1 on our cells. While our cells were positive for PECAM-1 (Figure 2A), PECAM-1 is also expressed by monocytes, keratinocytes, trophoblasts, and leukocytes[7]. VE-cadherin is one of the few proteins expressed ubiquitously throughout the endothelium[71], and presents on very few other cells in the body, possibly limited to trophoblasts and fetal stem cells[7]. Its importance has been shown in that disruption of VE-cadherin can cause embryonic lethality in gene knockout[72]. This makes VE-cadherin an excellent EC marker; the presence of VE-cadherin should exclude all cell types except endothelial cells and stem cells. Our cells were positive for VE-cadherin (Figure 2B). vWF is predominately made

by endothelial cells and megakaryocytes. While different factors can upregulate vWF, its presence is a good EC marker[73,74]. ICC reveals a dense presence of vWF, it appears secretion of vWF can be observed as well by the seemingly extracellular presence of vWF (Figure 2C). High levels of acetylated low-density lipoprotein (Ac-LDL) uptake is also a well-known marker[75,76] and was observed in our cells (Figure 2D). The lectin *Griffonia simplicifolia* IB_4 (GS-IB_4) is another marker commonly observed in endothelial cells,[77] which can be used for EC selection and isolation[11,78]. Our cells have a dense expression of GS-IB_4 (Figure 2E). Finally bright-field (or phase-contrast) microscopy was used to observe whether the cells created tube-like structures when grown on Matrigel® (Figure 2F). Tube formation is a quick way to observe the pathways and/or genes involved in angiogenesis. Endothelial cells should naturally form tubular structures, much like capillaries[79] especially when Matrigel® is used as the subcellular matrix. As seen in Figure 2F our cells formed tubular structures when Matrigel® was substituted for gelatin.

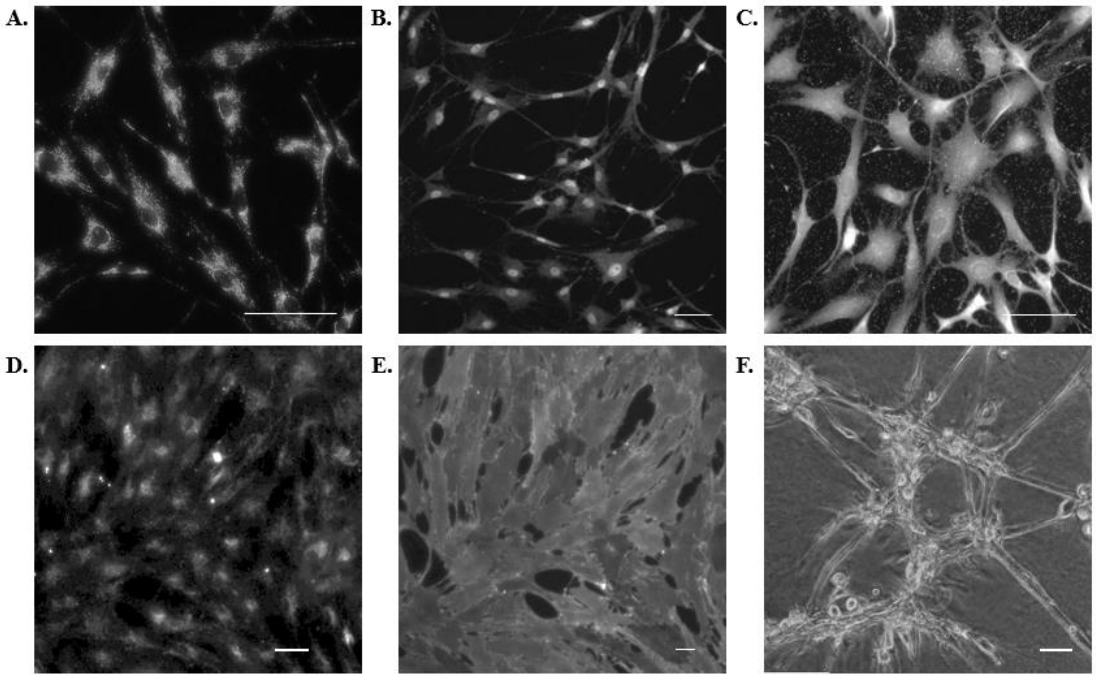

Figure 2. Identification of endothelial cells. Immunofluorescence staining of primary endothelial cells (A-E). ECs are representative of all sex and vessel origin. Scale bar, 50 μm (A-F). Classic EC markers are used for A-C: PECAM-1 (A), VE-cadherin (B) and vWF (C). Uptake of acetylated-low density lipoprotein (Ac-LDL) (D). Presence of lectin, *Griffonia simplicifolia* IB_4 (GS-IB_4) (E). Bright-field microscopy was used to visualize tube formation (F).

After harvested cells were identified as EC, we also needed to confirm their sex. To do this we used the testis-determining factor (TDF), which is also known as the sex-determining region Y (SRY) protein[80]. This protein has been used successfully to identify male cells in the body by using Real-Time Quantitative Reverse Transcription (qRT-PCR) and traditional PCR gel [11,81]. A representative image (Figure 3) shows the presence of SRY protein in both male ECs (aorta and SKM), while the female clearly lacks the SRY protein. Actin was used as a loading control, and sterile H_2O was used as a negative control in Figure 3.

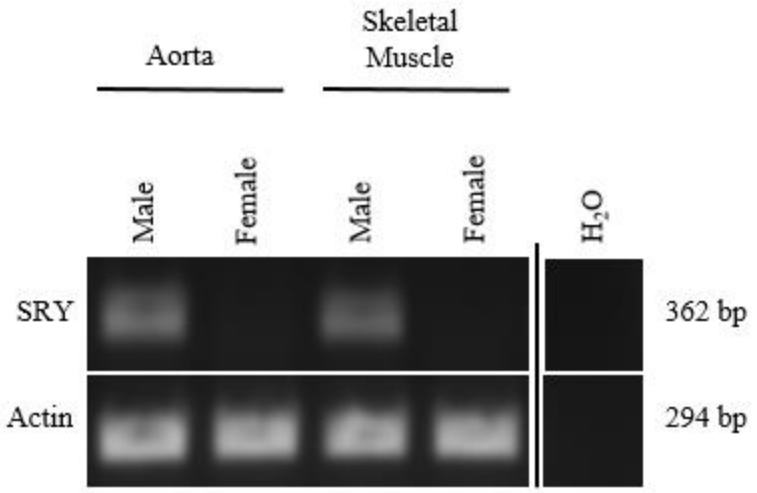

Figure 3. Confirmation of Cell Sex. Using qRT-PCR male sex was confirmed from the presence (male) or absence (female) of the sex-determining region Y (SRY) protein. Actin was used as a loading control and sterile H_2O was used as a negative control.

Our next goal was to measure quantitatively the size and diameter of ECs (Figure 4: MA (solid blue), FA (solid magenta), MS (striped blue) and FS (striped magenta)). In Figure 4A and 4B the data are represented using a box and whisker format with median being the center line, the 25th percentile being the bottom of the box, the 75th percentile being the top of the box, and the bottom and top whiskers extending to the 5th and 95th percentile range of data, respectively. Bars above the data indicate a significant sex difference within vessel origin (sex difference = black), bars below the data indicate a significant difference between vessel origin (vessel origin difference; male = blue, female = magenta). Data were collected for Figures 4A and 4B, and normality was tested using Anderson-Darling test. Normality was rejected for all data. Because of this, comparisons

for Figures 4A and 4B used non-parametric Wilcoxon Rank Sum Test for independent sample and non-normal distributions; confidence interval 95% (alpha = .05).

In Figure 4A, the median diameters of MA (n=1669), MS (n=2300) and FS (n=1758) were found to be ~16 μm and the diameter of FA (n=1825) was ~14 μm. Significant sex differences were observed between MA and FA ($P<.05$) but not between MS and FS ($P = .32$). With respect to vessel origin differences both MA and MS as well as FA and FS differed significantly ($P<.05$). Given the similarities between medians, it is important to note that Wilcoxon Rank Sum Test takes into account the population distribution, which is why MA and MS were found to be significantly different, despite the apparently same median diameter.

In Figure 4B, surface area of cells were measured using IHC of β-tubulin. Cells were attached to plate, then cells areas were measured using Image J (NIH)[67] and Leica TCP SP8 MP microscope in the Molecular Cytology Core of the University of Missouri-Columbia. Medians of values were calculated for all four cell types: MA ~575 μm^2 (n = 119), FA ~660 μm^2 (n = 119), MS ~860 μm^2 (n = 119) and FS ~950 μm^2 (n = 119).

Significant sex differences were observed between MA and FA ($P=0.02$) but not between MS and FS ($P=0.13$). Significant vessel origin differences were observed between both MA and MS ($P<.05$) and between FA and FS ($P<.05$).

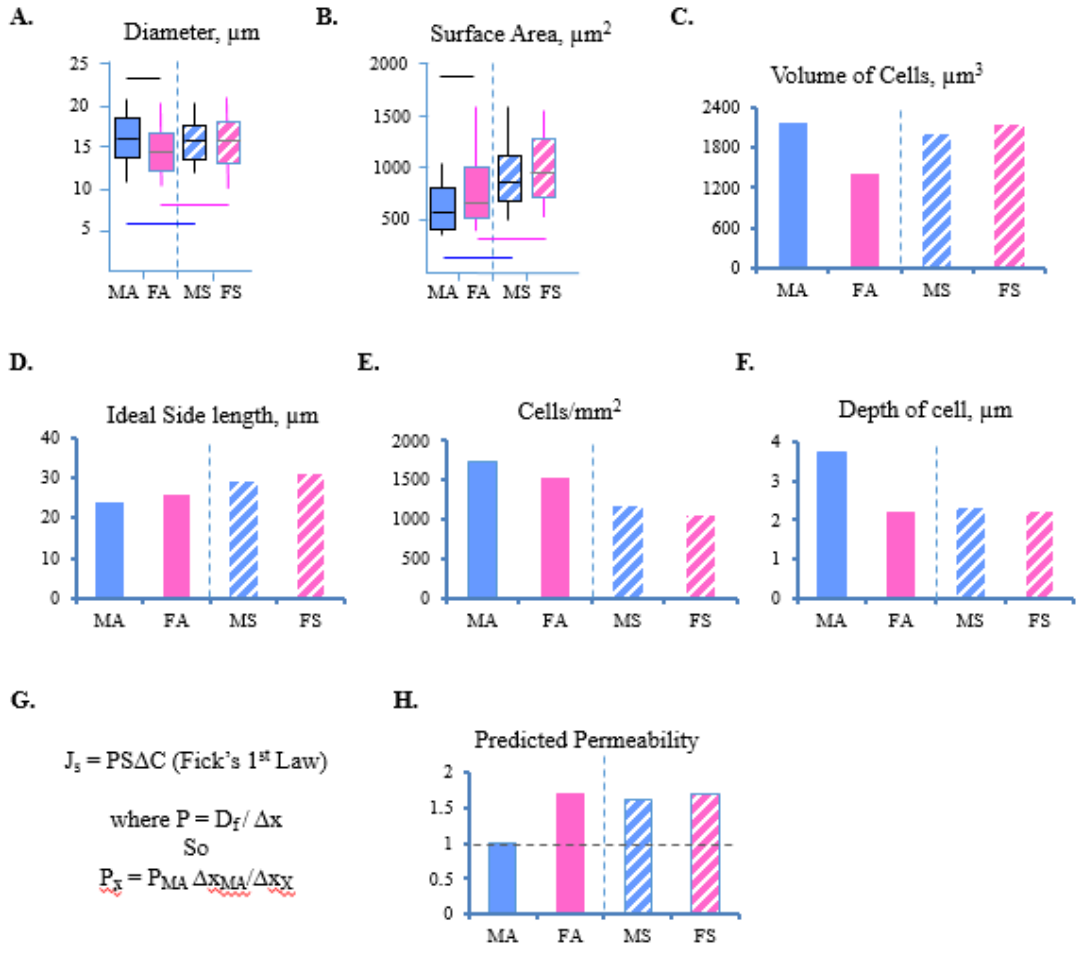

Figure 4. EC size, shape and predictions. MA = male aorta EC (solid blue), FA = female aorta EC (solid magenta), MS = male skeletal EC (striped blue) and FS = female skeletal EC (striped magenta). Black bars above cell types indicate significant differences between sexes ($P < .05$), a blue bar below data indicates a significant difference between male aorta and male SKM ($P < .05$), a pink bar below the data indicates a significant difference between female aorta and female SKM ($P < .05$) . Diameter of freely suspended cells in µm (A). Surface area of attached cells in μm^2; MA, FA, MS, FS each had n=119 (B). Calculated volume of cells in μm^3 based on diameter; MA: n=1669, FA: n=1825, MS: n=2301, FS: n=1758 (C). Ideal Side length in µm based on surface area if the EC were a perfect square (D). Cells per mm^2 calculated from surface area (E). Depth of cells in µm, calculated from volume and surface area (F). Formula of Fick's 1st Law, in relation to permeability (G). Predicted permeability calculated using cell depth and Fick's 1st Law.

Growth rates were measured using CyQuant® Cell Proliferation Assay Kit (Molecular Probes®, Life Technologies). Experiments were performed in triplicate using the 4 cell types (MA, FA, MS, FS, respectively). Because seeding densities differed slightly, the data were normalized to the actual initial density and reported as fold-increase. By day 6, FA had increased by 5.0-fold, while MA had increased 6.7-fold (Figure 5A). By day 6, FS cell number had increased by 7.4-fold, while MS had increased by 20.5-fold (Figure 5B).

For a statistical analysis of these data: individual growth models for exploring longitudinal data on wells over time was used. The structure of the variance-covariance matrix of the repeated measurements was also analyzed and entered in the model.[5] As shown in Table 1, a mixed model with a random linear and quadratic effect provides a significantly better fit than the model with the random linear component alone. Adding a cubic component did not significantly improve the fit of the model (data not shown). Quadratic Growth models with grouping variables of sex or vessel origin provide an even better fit, indicating that female cells grow at a different rate than male cells, and aortic cells grow at a different rate than SKM ECs. Moreover, the overall fit of the Quadratic Growth Model grouped by sex and vessel origin confirms a significant difference in growth between sex within vessel origin, and difference between cells type within sex. This indicates that growth patterns are significantly different between each group MA, FA, MS and FS. A general trend observed seems predictive ability of ECs grouped by: General continuous EC< By Sex < By Vessel Origin < Sex and Vessel Origin.

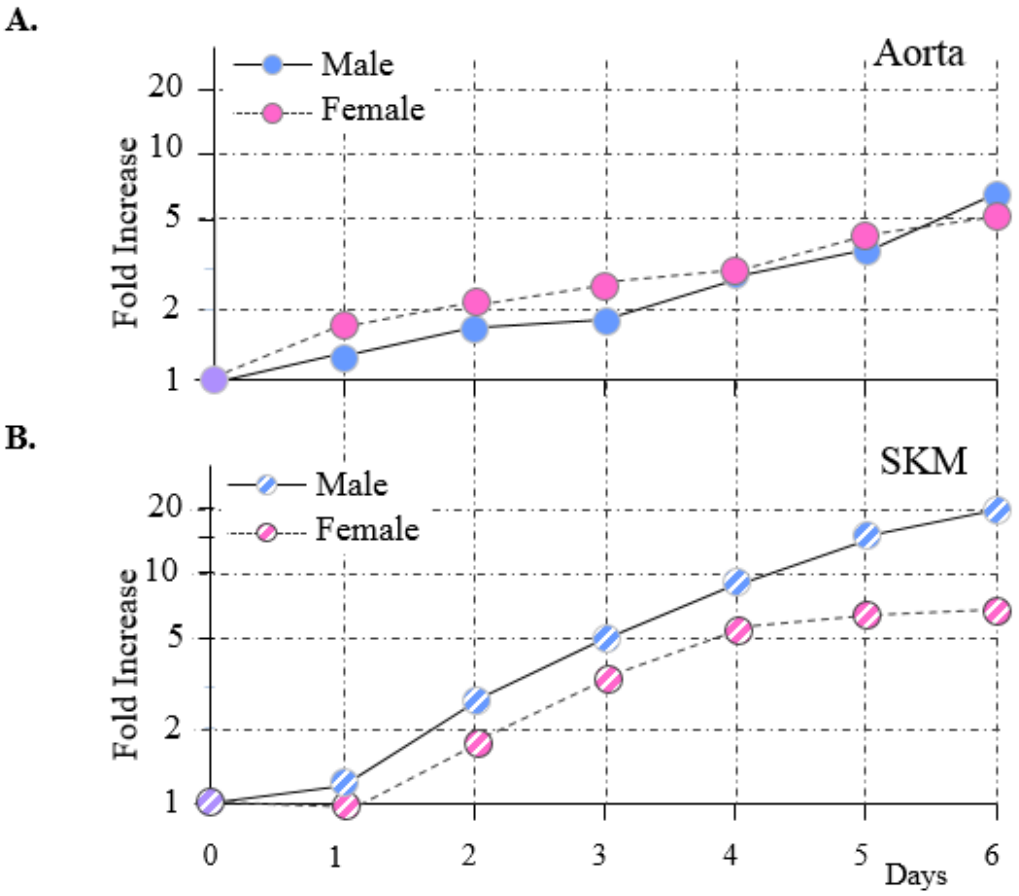

Figure 5. Growth rates in cell culture. Above are growth rates, quantified using a cell proliferation kit. Growth rates of male and female aortic EC are observed to have similar growth patterns (A). While male and female SKM EC seem to have very different growth rates, with males seeing a ~20 fold increase (B). All cell types were grown at same time, in same conditions, therefore, cells in figure A and B can be compared to one another. Values are means of experiment performed in triplicate.

Table 1. Unconditional Growth Models: Parameter Estimates and Model Comparisons

	Parameter Estimates			Fit Statistics		
Model	Intercept	Day	Day*Day	AIC	BIC	-2RLL
Linear	-502.91	1950.52**	-	1533.1	1538.1	1333.1
Quadratic	855.73	320.15	271.73*	1404.3	1405.7	1398.3
Quadratic V-C Grouped by Sex	855.73	132.56	83.22**	1389.7	1391.2	1383.7
Quadratic V-C Grouped by Vessel Origin	855.73	199.46	75.80*	1386.5	1388.5	1378.5
Quadratic V-C Grouped by Sex and Vessel Origin	855.73	620.18**	149.47**	1390.7	1394.1	1376.7

*p<.05 ** p<.001; AIC = Akaike information criterion; BIC = Bayesian information criterion; -2RLL = -2 times the difference between their residual log likelihoods.

The original approach was to use immunocytochemistry (ICC) to compare relative protein expressions by EC tissue and sex, however multiple concerns arose. As illustrated in Figure 6A using NCAD protein expression as an example, quantifying protein expression per cell can be tricky. Although similar cytosolic protein expression is observed in all cell types (MA, FA, MS and FS), cell density appears to influence protein expression. Furthermore, the area of cells that can be imaged at any one time represents a small area relative to the whole plate. It is likely that the group of cells in the field of view are clones of one another, due to seeding, and may not provide an accurate representation of the entire population (plate). Identifying the edges of the cells can also be difficult, as density varies from cell type to cell type. Finally, it is difficult to precisely

identify a cell free area to subtract out as a negative control, which we have found to have vessel origin and sex differences (Figure 1). Consequently, we decided to use flow cytometry (Figure 7) to compare protein expression between cell types as a larger number (tens of thousands vs. hundreds) of cells can be sampled with greater precision.

That said, we did observe sex differences using ICC which would not be recognized using flow cytometry. In Figure 6B, ERβ location varies greatly by sex. In aorta and skeletal muscle EC from males ERβ is completely cytosolic and perinuclear, with little expression in the nucleus. By contrast, ER β in aorta and SKM EC of females is primarily in the region of the nucleus. These results were also recapitulated in EC of the mesentery (data not shown). Receptor location sex differences were not observed in ER-α or AR. Figure 6 scale bar = 50 μm.

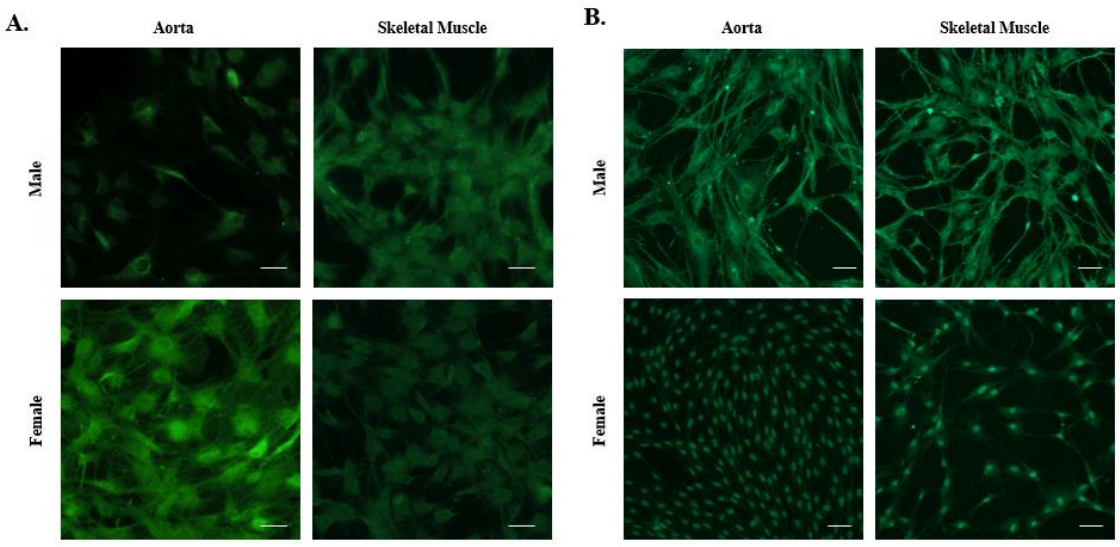

Figure 6. Immunocytochemistry (ICC). Cell types were grown and stained for NCAD expression (A). Cell types were grown and stained for ERβ (B). Interestingly, there seems to be a receptor location difference based on sex. In male cells, ERβ is primarily cytosolic and perinuclear. In contrast, female cells are observed to have a predominately nuclear expression of ERβ. Scale bar, 50 μm.

Given our concerns about using ICC for quantitative measures, we instead chose to measure protein expression with flow cytometry. Using techniques described in our methods section (Figure 1), we averaged the duplicate flow cytometry results per vessel origin and sex type, then compared them to other vessel origin and sex types (i.e. MA, FA, MS, and FS). Whichever group had the highest set of protein expression was set to 100% with the remaining groups referenced to that in the form of a heat map (Figure 7).

Our next goal was to elucidate possible inherent differences in protein expression. We divided these into four sections: sex hormone receptors, WBC-EC adhesion, EC junctional proteins and EC-ECM proteins (Figure 7).

Sex hormone receptors – It was logical to determine whether the 3 primary sex hormones receptors, AR, ERα and ERβ , were present on the EC and whether they differed by sex and/or by vessel origin. Overall, protein expression of AR, ERα, and ERβ was highest in MA while in FA almost no AR was present. Figure 7 illustrates the relative expression of the proteins.

EC Junctional Proteins - From our data, PECAM-1 expression in the cells from females is significantly higher than that of the cells from male in either tissue. VE-CAD is a junctional protein as well, which is known to be an integral component of vascular permeability[71]. We find that, for both sexes, the EC from aorta have higher expression of VE-CAD than those from SKM.

EC-WBC adhesion – Given that inflammation is associated with loss of barrier function, chronic inflammation can result in interstitial edema and disease progression, and that

inflammatory process may differ by sex[82,83], it stands to reason WBC-EC adhesion proteins might provide a clue about the basis for sex differences in inflammatory states. We find that ICAM-1 varies by EC vessel of origin, with much higher protein expression in EC from aorta than SKM microvessels, while VCAM-1 varies by sex, wherein protein expression in males exceeds that of the females.

EC-ECM - The NCAD result is intriguing as its expression was higher in the EC from females relative to the males and it is a cadherin whose function in EC is not fully understood. $\alpha_v\beta_3$ was similar in ECs from Aorta of both sexes and in ECs from female SKM; of interest, its expression was significantly lower in MS microvessels.

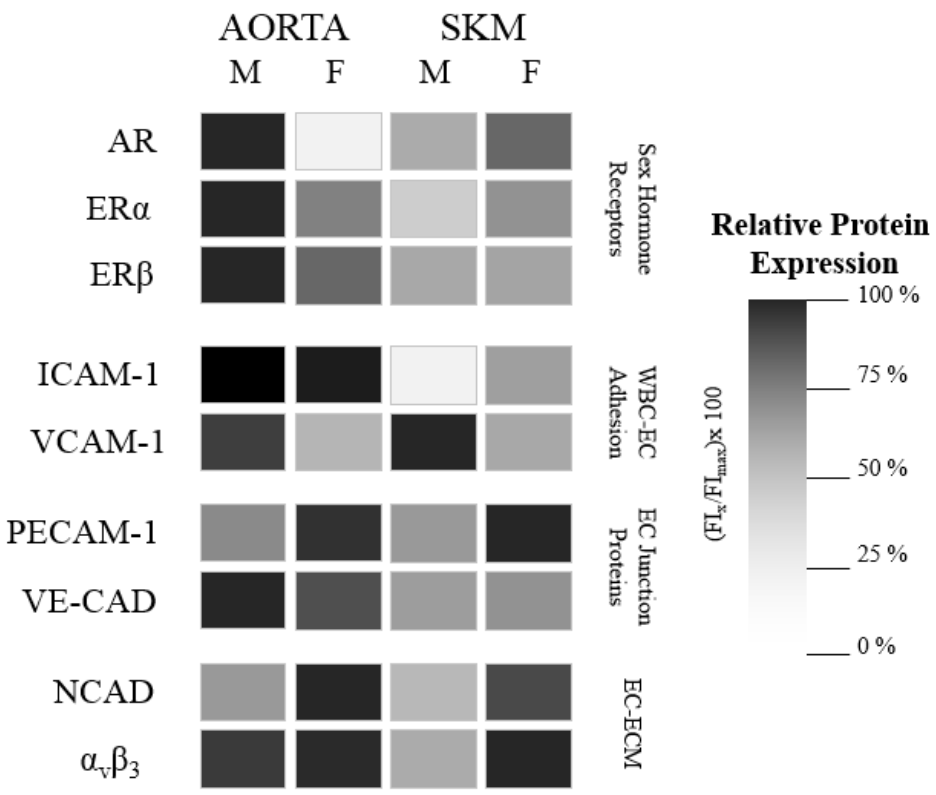

Figure 7. Heat-map of selected EC protein expression. A heat map was created to view relative protein abundance between different EC of both sexes derived from aorta and from skeletal muscle. M = male, F = female. FI_x = Fluorescent intensity of a cell type, FI_{max} = Fluorescent intensity of cell type with highest protein expression. On far right is a legend of relative protein expression. Values are means of experiments performed in duplicate.

Breaking the heat-map apart from Figure 7 into male vs. female for both aortic macrovessel and SKM microvessel ECs, we can more easily see general trends in the data. Figure 8 is a graph scaled to the log(10), for the purpose of limiting the power of observed differences. The blue illustrates male protein expression in excess to female, magenta illustrates female protein expression in excess of male. The red line at 0.3, equals to a two-fold change, and is given as a point of reference. When considering aortic macrovascular EC (Figure 8A), protein expression of PECAM-1 and NCAD

predominates in the cells from females. No real sex difference is apparent for either ICAM-1 or $\alpha_v\beta_3$; and VCAM-1, VE-CAD and the steroid receptors are expressed to a greater extent in cells from the males. In contrast the expression profile differs significantly in the SKM (Figure 8B), wherein only VCAM-1 favors male in protein expression.

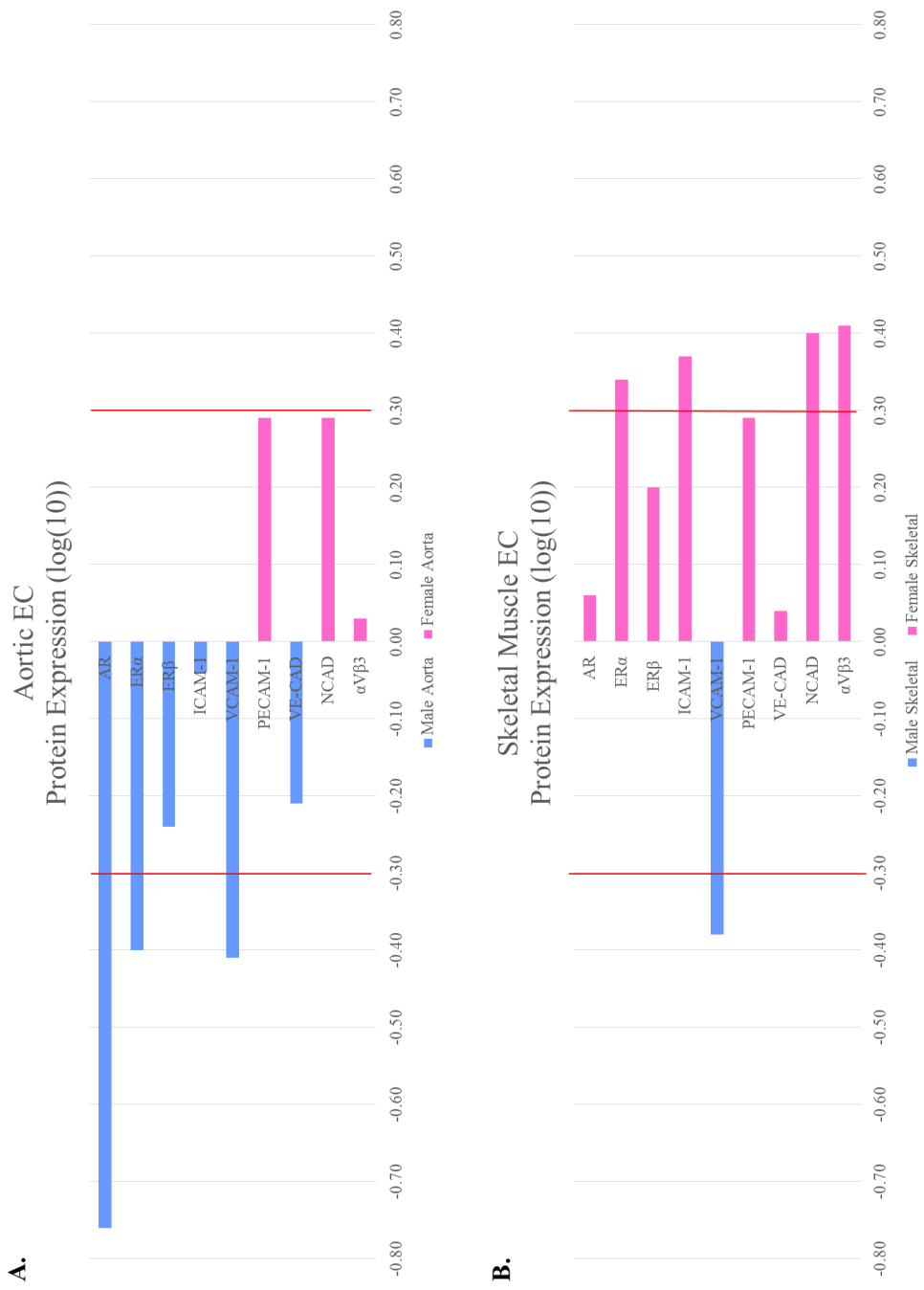

Figure 8. Sex differences between aortic (macrovessel) and skeletal muscle (microvessel) protein expression. Magenta protein expression on the right indicates female protein expression is higher. Blue protein expression on the left indicated male protein expression is higher. Protein expression is represented to the log(10). The red lines at .3log(10) represent a two-fold protein increase (arbitrarily chosen as our point of significance). 0 in the middle indicates protein expressions are equal (present in 1/1 ratio). Relative protein expression is compared between Aortic EC of male and female

rats (A). Relative protein expression is compared between SKM EC of age-matched male and female rats (B).

To investigate the similarities and differences in our target protein expression the data in Figure 7 were reanalyzed. First the data were grouped by sex without regard to vessel of origin (Figure 9A). Second, the data were grouped by tissue of origin (also representing macro- vs microvascular EC; Figure 9B). Colors for Figure 9A were darkened to indicate the combined groups. Dark blue = favors male protein expression, dark magenta = favors female protein expression. In Figure 9B yellow favors aortic protein expression, green favors SKM protein expression. The red line at 0.3 is represents a two-fold change. When looking at overall sex differences (Figure 9A), we see PECAM-1, NCAD and $\alpha_v\beta_3$, ICAM-1, and ERβ was greater in female EC protein expression; and VCAM-1, AR, ERα and VE-CAD was greater in male ECs. With respect to vessel origin difference in the absence of sex (Figure 9B), only VCAM-1 favors SKM in protein expression, while AR is has no difference.

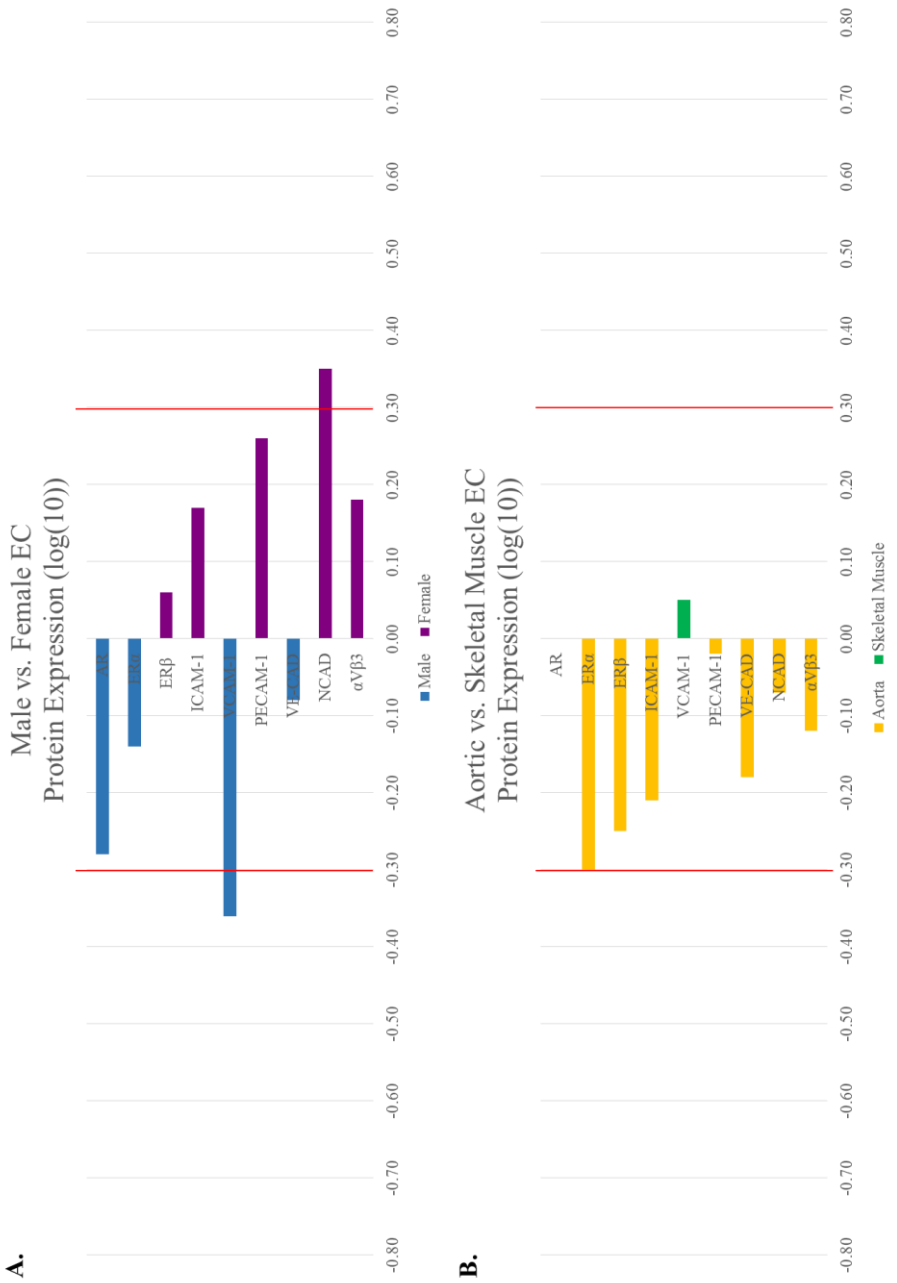

Figure 9. Target protein expression by sex and by vessel origin: Summed differences of sex (aorta + SKM) and vessel origin (male + female). Dark magenta protein expression on the right indicates female (sum of FA + FS) protein expression is higher. Dark blue protein expression on the left indicates male (sum of MA + MS) protein expression is higher (A). Green protein expression on the right indicates SKM (sum of MS + FS) protein expression is higher. Gold protein expression on the left indicates male (sum of MA + FA) protein expression is higher (A). Protein expression is represented to the log(10). Red lines at .3log(10) = a two-fold protein increase (arbitrarily chosen as our point of significance). 0 in the middle indicates protein expressions are equal (present in a 1/1 ratio).

DISCUSSION

The primary purpose of this study was to determine whether it was appropriate to assume that continuous, non-fenestrated ECs do not differ by either tissue of origin or by sex, as predicted by our hypothesis. The pronounced outcome of the studies was outright rejection of our initial hypothesis as the sex, of the strain- and age-matched rat from which the EC were harvested, influenced multiple parameters even in the face of being handled/exposed to constant, identical conditions of culture.

One way to evaluate the viability of our results is to compare characteristics of our cells to characteristics ascribed to EC in the current literature. According to Figure 2, our cells exhibit the classic markers of ECs, as well as identifying with the correct sex (Figure 3). In Figure 4, we measured cell surface area and cell diameter. Our surface areas ranged from 575-950 μm^2. According to one paper, *in vivo* mouse ECs in skeletal muscle (cremaster) arterioles were ~1200 μm^2 in surface area, and those in the venules were ~600 μm^2 in surface area.[51] Our microvascular ECs fell directly between the two observed values: MS = 860 μm^2 and FS = 950 μm^2. It stands to reason that our ECs may possess an 'average phenotype' as they were derived from a mixture of arterioles, venules and capillaries that can then differentiate based on micro-environmental cues. Another source states human ECs are typically 50-70 μm long and 10-30 μm wide and 0.1-10 μm deep[5]. If we assumed the cells were elliptical and use the smallest and largest combination of dimensions the calculated area would range from ~290 μm^2 to ~1650 μm^2. Our ECs fall in this range for size and depth.

The measured values of EC diameter and surface area were used to calculate several other factors including EC volume (calculated from diameter (Figure 4C) assuming spherical cells). The ideal side length from surface area shaped as a square (Figure 4D). EC surface area could be used to calculate the cells existing in a square millimeter (Figure 4E). Depth could also be calculated from surface area and volume (Figure 4F), and predicted permeability calculated using cell depth (Figure 4H) in the Fick Equation (below). These are of course over-simplifications, as cell depth will vary from point to point in an EC, and ECs do not orient into perfect rectangular cuboidal shapes. These may be further skewed by EC surface area measurements looking at individual cells that are not in contact (or very little contact) with other cells, as they normally exist in a confluent state. Finally, we are assuming the diameter of the cells is spherical, and not being compressed if cell descends to the bottom. With these caveats in mind, the calculations allowed us to make interesting inferences about the cells, especially in regards to relative permeability.

To calculate the relative permeability of the ideal EC monolayer (Figures 4G and 4F), we used Fick's first Law, $J_S=PS\Delta C$ where J_S is flux of solute (mmole s^{-1}), P is the diffusive permeability coefficient (cm s^{-1}), which is defined as $D_f/\Delta x$, where D_f is the free diffusion coefficient of the solute (cm^2 s^{-1}) and Δx is the thickness of the barrier (cm). Because the independent variable in diffusive permeability is cell thickness, we can rearrange the equation[26], leaving us with a ratio with which the P of one cell type can be compared to that of another: $P_x = P_{MA}$ (all cell types will arbitrarily compare to male aorta) $\Delta x_{MA}/\Delta x_x$. Thus, permeability to water-soluble solutes of MS is predicted to be ~1.6-fold higher (leakier) and FA and FS ~1.7-fold higher than an idealized monolayer of MA

(Figure 4H). Interestingly, due to the greater number of cells present in 1 mm^2 in MA compared to FA (Figure 4E), one would predict the P_{MA} to be greater than P_{FA}. The increased thickness of the MA may be a compensatory mechanism to reduce P.

After examining the cell diameter and surface area data, we determined whether there were differences between our cohorts of ECs with respect to growth. Generally, microvascular MS ECs grew at a significantly faster rate than FS or ECs from aorta of either sex. Given that human males have a greater muscle mass (both absolute and relative) than females[84], it is possible that the faster EC SKM growth rates are a basis for sexual dimorphism. Juvenile microvascular FS ECs have also been observed to grow more slowly than juvenile MS ECs (data not shown). Another general observation warranting discussion is, despite being grown in the constant environmental conditions of an incubator, it appears that EC from males have reduced rates of growth in the summer months while EC from the females (aorta specifically) grow more quickly in the summer months (data not shown). Is there an annual circadian rhythm that drives the cells despite being in a room artificially lit, and in a fairly stable temperature and humidity? There are data from the laboratory demonstrating yearly patterns of basal microvascular hydraulic conductivity in frog mesenteric capillaries (males)[85]. Annual EC growth rates of this cohort would be an interesting experiment for the future.

Our next goal was to evaluate protein expression by the cells. We first tried ICC, however, problems comparing multiple groups quickly became apparent. Instead, flow cytometry proved to be more useful tool to evaluate protein expression per cell given that larger populations of cells could be analyzed at one time. However, ICC did yield interesting data as illustrated in Figure 6B. In this case we find that the distribution of the

ERβ protein varied by sex. At this point in time we are not sure what to make of male ERβ being almost completely cytosolic, and female ERβ being almost exclusively nuclear, however, we believe this could have implications as to the function of these receptors. These pronounced differences in distribution were not observed for the other hormone receptors (or other proteins) probed in this study. Again, in future it would be interesting to probe the downstream signaling pathways associated with ERα and ERβ in ECs from each sex to determine whether the cytosolic relative to nuclear distribution of ERβ is responsible for putative sex-related differences in function.

In Figures 7, 8, and 9, we examined target proteins and obtained several interesting results:

The junctional proteins we investigated in this thesis included PECAM-1 and VE-CAD. PECAM-1 could be classified as a EC-WBC protein as well, however, we felt PECAM-1 was more of a junctional protein for our purposes.[46] PECAM-1 expression was observed to differ by sex. Males had roughly half the PECAM-1 expression as females (Figure 7). It is possible these sex differences could be linked to barrier function in addition to sex-differences in immune function. By using different mechanisms to achieve the same goal, male and female immune systems would react differently to different stimuli and could offer an explanation as to why clinicians observe differences in proportions of males and females affected by different diseases[18,21]. Unlike PECAM-1, VE-CAD expression was vessel origin-linked, i.e. more regulation in the aortic ECs (Figure 7). This up-regulation may be due to cell thickness (in the case of MA Figure 10), or to decrease of permeability to macromolecules in the aorta. As VE-CAD is

involved in regulating paracellular transportation, it would be interesting if there was a decrease in intracellular transportation in the macrovascular EC as well.

The expression patterns of the cell adhesion molecules ICAM-1 and VCAM-1 differed. Notably, ICAM-1 expression appears to be dictated by site along the vascular tree, while VCAM-1 is dictated by sex (Figure 7). Given our EC spreading data, and the abundance of protein expression, a sex- and vessel location difference in EC-leukocyte interactions would be predicted favoring greatest leukocyte interaction with male aorta and least with female microvascular SKM EC. Given the increased density of VCAM-1 on male EC (Figure 7) and given that VCAM-1 is tied to early stages of atherosclerosis, these findings are consistent with the clinical observation that males are more prone to developing atherosclerosis than females[54]. Finally, because of the relatively high levels of ICAM-1 on the aortic EC and that a group found sICAM-1 to be a better indicator of their microvessel[57] line it would be interesting to determine whether our microvessel EC were generating sICAM-1. Activation of MMPs in the culture media would reduce ICAM-1 expression on SKM microvascular EC compared to the macrovascular EC of the aorta.

The only integrin we investigated was $\alpha_v\beta_3$, which has been tied to EC growth. Because $\alpha_v\beta_3$ expression is linked to cell growth[66] the relatively low levels of expression detected in male SKM ECs are consistent with the finding that the EC of male SKM grow much faster than all other cell types (Figure 5). Because of this, it may not be surprising that as the male SKM reach confluence earlier than the other cells that they would have down-regulated $\alpha_v\beta_3$ expression.

NCAD is an interesting protein known to interact with the ECM and perivascular cells, specifically pericytes[59,65]. Given that the contribution of NCAD to EC function has yet to be elucidated, it is interesting we find its expression to be sex-linked, with a much higher content in the ECs from the females. If these data are recapitulated *in vivo*, it may be possible to gain a better understanding of NCAD's function via understanding the mechanisms determining the sexual dimorphism we observe.

Finally, we sought to summarize these data into an easy to understand cartoon. The cartoon in Figure 10 is a 2-D representation of our surface area/cell thickness data, merged with a simplification of the protein expression data. Relative depth and spreading are drawn to scale based on our calculations. Proteins being investigated were clumped together for simplicity's sake. Junctions were "enlarged" to show the adherens junctional proteins we investigated. The Key for the proteins investigated is on the far left; the aortic cells are the solid colors while the SKM cells are striped (in both blue depicts males while pink denotes females).

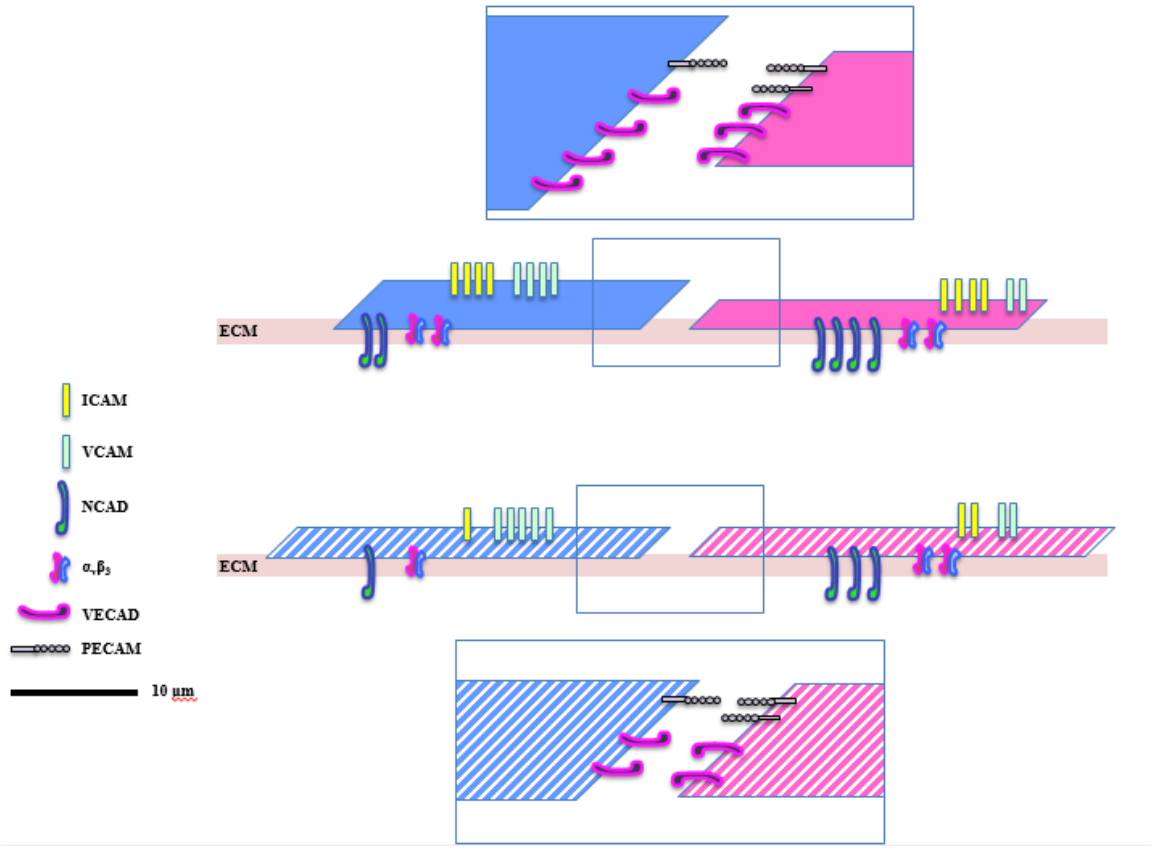

Figure 10. Cartoon representation of EC protein expression and size illustrating the influence of tissue origin and sex. Solid colors are the macrovascular EC and striped the microvascular EC. Solid blue indicates male aortic EC, solid magenta indicates female aortic EC, striped blue indicates male SKM EC, and striped magenta indicates female SKM EC. Cells are drawn to show calculated length of one side and cell depth in a simplistic model from figure 4. Using heat map from figure 7, rough approximations were made at whole number protein expressions. Cell junctions were enlarged to view junctional proteins. Scale bar, 10 µm.

Endothelial cell culture in this study allowed large populations of cells to be grown under identical conditions; and analyzed in tandem. However, cell culture has disadvantages that preclude a direct application of the outcomes to the understanding of the intact vasculature. As cells are passaged they tend to lose their *in situ* "identity"[5], meaning the ECs tend to behave less and less like ECs *in vivo* as time goes on. In addition, EC culture uses an artificial environment that only approximates *in vivo*

conditions. Because ECs are not exposed to their normal environmental cues of flow, pressure, fluctuations in concentration, transvascular exchange, stimuli, etc., it is hard to gauge how well our results represent the extent to which the differences reported in this thesis would be observed in a live animal. Nevertheless, and perhaps the most exciting of this thesis, is that these ECs do act differently under identical carefully controlled environmental conditions. It is amazing to see things like cell spreading Figure 4B, differs by vessel origin, or aortic cell size (Figure 4A) differs by sex. Completely unexpected was the very clear sex difference in location of receptor expression of ERβ in Figure 6B.

The growth modeling analysis elucidated an interesting outcome demonstrating a hierarchy of importance of variables: Random Continuous EC < Grouping by Sex < Grouping by Vessel Origin < Grouping by Sex and Vessel Origin (Table 1). When we take these results and look at cell spreading and cell diameter the same hierarchy appears (both with respect to spreading and to diameter), differing significantly by vessel origin in males and females, but only aortic macrovascular EC differed significantly by sex (Figure 4A and 4B). Finally, when we examine the data in Figure 9, we observe several male/female sex differences, however, when comparing aortic EC (macrovessel) to SKM EC (microvaessel), we find almost every protein we investigated expression was greater in aorta. This makes sense as environment and function of the aorta differ profoundly from that of SKM microvessels. Several studies have documented multiple differences in EC phenotype by position in the vasculature (Macro- vs microvessel; arteriole vs capillary vs venule) and by organ[7]. Consequently we would expect ECs in the aorta to differ from ECs in the SKM more than we would expect to see differences between EC of

males and females. However, what we found was on a per protein basis, either sex or vessel origin could be more predictive of how that protein will be expressed.

An additional unknown of the culture condition is the composition of fetal bovine serum (FBS) in the media. Specifically, FBS contains unspecified levels of growth hormones and reproductive hormones; a logical next step would be to quantify which hormones/growth factors in the FBS to which our cells have been exposed. As it happens FBS from the same lot has been used throughout all of these studies. The presence of the reproductive hormones are believed to be major drivers in sexual dimorphism in humans and other mammals *in utero*. The sex hormones to be explored would be testosterone, estrogen, progesterone, along with their derivatives. These are present in varying amounts in both males and females. With respect to vascular function, given that low levels of testosterone have been shown in men to cause damage to the endothelium[40] it would be interesting to test how male ECs respond to cell media containing no testosterone versus normal levels of testosterone. For females, it would be interesting to do the same thing but with estrogens. Then it would be interesting to try testosterone on females and estrogen on males to determine if responses go be repeated, ultimately showing how ECs of different sex origin, reacted to different sex hormones. It could be very important to study vascular and endothelial function of the transgender population before and after sex change. An additional study that is needed is to determine whether these results recapitulate themselves *in vivo*.

It is fascinating to see the differences and similarities when looked at by either sex or vessel origin. Perhaps the most interesting trend in the data is the seemingly predictive

manner of how likely a cohort of cells is to represent a specific EC in the continuous endothelium (as mentioned above):

Random Continuous EC < Grouping by Sex < Grouping by Vessel Origin < Grouping by Sex and Vessel Origin

The idea this trend recapitulates itself both helps to validate the data, and shows why sex and vessel origin differences should not be a specific area of study, but rather should be present in all physiological/medical research, as a way to support rigor and reproducibility.

We observed differences in macro- and microvasculature, in two places covered by continuous endothelium (implying similarity). Based on our results, the use of human umbilical vein ECs (HUVECs) may be a poor choice to "represent" ECs, because our cells display characteristics based on where they came from (both genomic sex and site along the vascular tree) even after exposure to cell culture (*4.4 passages*). It is not known to what degree male and female ECs differ by sex hormone exposure, genomics, epigenetics, or micro-enviroment (e.g. diabetics, hypercholesterolemia, age, prevalence of fat, etc.). While similar questions could be asked regarding to what degree ECs differ by vascular bed of origin. What is clear is future studies will be necessary to elucidate sex differences and vessel origin differences in the endothelium, and the clinical implications these differences hold. In conclusion, our data show significant differences between male and female ECs, as well as significant differences between ECs originating from the micro and microvasculature.

Appendix-1

AIC = Akaike information criterion; BIC = Bayesian information criterion; -2RLL = -2 times the difference between their residual log likelihoods.

-2RLL - -2 times the difference between their residual log likelihoods.

Δx - Thickness of the barrier (cm)

AIC - Akaike information criterion

AR – Androgen receptor

$\alpha_v\beta_3$ – Alpha-v beta-3

BIC - Bayesian information criterion

D_f - Free diffusion coefficient of the solute ($cm^2\ s^{-1}$)

DPBS - Dubecco's Phosphate Buffer

EC(s) – Endothelial cell(s)

ED – Erectile dysfunction

ERα – Estrogen receptor alpha

ERβ – Estrogen receptor beta

FBS – Fetal Bovine Serum

FA – Female aorta

FS – Female skeletal muscle

HEPES - 4-(2-hydroxyethyl)-1-piperazineethanesulfonic acid

HBSS – Hanks' Balanced Salt Solution

HUVEC(s) - human umbilical vein endothelial cell(s)

ICAM-1 - intercellular adhesion molecule 1

J_S - Flux of solute (mmole s^{-1})

MA – Male aorta

MS – Male skeletal muscle

NCAD – N-cadherin or neural cadherin

P - Diffusive permeability coefficient (cm s^{-1})

PECAM-1 – Platelet endothelial cell adhesion molecule

s(ICAM-1) – Soluble ICAM-1

s(VCAM-1) – Soluble VCAM-1

SKM – Skeletal muscle (derived from abdominal free wall)

SRY Gene – Sex-determining region Y gene

VCAM-1 - Vascular cell adhesion protein 1

VE-CAD – Vascular endothelial cadherin, CD144

Appendix – 2

Gelatin

Gelatin from bovine skin – 0.2% w/v gelatin in DIH_2O. Autoclave.
(Sigma-Aldrich, St. Louis, MO)

TCB#1 (500 ml)

495 ml DPBS (Dubecco's Phosphate Buffer Saline) (1x) (-) Calcium Chloride
(-) Magnesium Chloride
(Gibco® | Thermo Scientific, Waltham, MA, USA)
625 µl Gentamicin
(Fresenius Kabi USA, Lake Zurich, IL, USA)
5 ml Amphotericin B (2.5 µg/ml)
(Gibco® | Thermo Scientific, Waltham, MA, USA)

TCB#2 (2x500 ml)

475 ml HBSS (1x) (-) Calcium Chloride
(-) Magnesium Chloride
(-) Magnesium Sulfate
(Gibco® | Thermo Scientific, Waltham, MA, USA)
625 µl Gentamicin
(Fresenius Kabi USA, Lake Zurich, IL, USA)
5 ml Amphotericin B (2.5 µg/ml)
(Gibco® | Thermo Scientific, Waltham, MA, USA)
5 ml GlutaMAX-1™-I (100X)

(Gibco® | Thermo Scientific, Waltham, MA, USA)

5 ml Sodium Pyruvate (100mM)

(Gibco® | Thermo Scientific, Waltham, MA, USA)

10 ml HEPES (1M)

(Gibco® | Thermo Scientific, Waltham, MA USA)

TCB#1A (20 ml)

18 ml TCB#1

2 ml Fetal Bovine Serum (FBS)

(F6178 | Sigma-Aldrich, St. Louis, MO)

TCB#3 (600 ml)

540 ml TCB#2

60 ml Fetal Bovine Serum (FBS)

(F6178 | Sigma-Aldrich, St. Louis, MO)

Flasks

Tissue Culture Flasks 25 cm^2 and 75 cm^2 with filter screw top flasks were used for all cell culture.

(TPP Techno Plastic Products AG, Trasadingen, Switzerland)

Flasks were always pre-coated with 0.2% gelatin for 30 minutes at 37°C, allow to air dry.

Freezing solution

Fetal Bovine Serum (FBS)

(F6178 | Sigma-Aldrich, St. Louis, MO)

10% Dimethyl Sulfoxide ≥99.9%

(Sigma-Aldrich, St. Louis, MO)

Trypsin

TrypLE™ Express (-) Phenol Red

(Gibco® | Thermo Scientific, Waltham, MA, USA)

Cell Media + 20% v/v FBS

375 ml M199 (1x) (+) Earle's Salts

(+) L-Glutamine

(+) 2.2g/L Sodium Bicarbonate

(-) Phenol Red

(Gibco® | Thermo Scientific, Waltham, MA, USA)

100 ml Fetal Bovine Serum (FBS)

(F6178 | Sigma-Aldrich, St. Louis, MO)

5 ml Endothelial Cell Growth Supplement (10 mg/ml)

(Corning, Bedford, MA, USA)

5 ml Sodium Pyruvate (100mM)

(Gibco® | Thermo Scientific, Waltham, MA, USA)

5 ml GlutaMAX-1™-I (100X)

(Gibco® | Thermo Scientific, Waltham, MA, USA)

5 ml Heparin (500 U/ml) – Heparin sodium salt, Grade I-A: From Porcine Intestinal Mucosa

(Sigma-Aldrich, St. Louis, MO, USA)

5 ml Amphotericin B (2.5 µg/ml)

(Gibco® | Thermo Scientific, Waltham, MA, USA)

625 µl Gentamicin

(Fresenius Kabi USA, Lake Zurich, IL, USA)

Magnetic beads labeled with CD31

6 ml MagnaBind™ Goat Anti-Mouse Magnetic Beads

(Thermo Scientific, Waltham, MA, USA)

Wash three times with 6 ml TCB#1A . Then add 6 ml TCB#3 and 60 µl CD31 antibody (see Antibodies), let incubate for 30 minutes at room temperature. After incubation, was three more times with 6 ml of TCB#3. Add 6 ml of TCB#3 and store at 4°C.

Digestive Enzyme Cocktail

20 ml TCB#2

0.060 g Collagenase IV

(Worthington Biochemical Corporation, Lakewood, NJ, USA)

0.002 g Deoxyribonuclease I

(Worthington Biochemical Corporation, Lakewood, NJ, USA)

48 U (0.0077 g) Neutral Protease Purified, AFO

(Worthington Biochemical Corporation, Lakewood, NJ, USA)

BIBLIOGRAPHY

1. Rajendran, P. *et al.* The vascular endothelium and human diseases. *Int. J. Biol. Sci.* **9,** 1057–1069 (2013).
2. Galley, H. F. & Webster, N. R. Physiology of the endothelium. *Br. J. Anaesth.* **93,** 105–113 (2004).
3. Vita, J. A. & Keaney, J. F. Endothelial function: A barometer for cardiovascular risk? *Circulation* **106,** 640–642 (2002).
4. Bianconi, E. *et al.* An estimation of the number of cells in the human body. *Ann Hum Biol* **40,** 463–471 (2013).
5. Aird, W. C. Spatial and temporal dynamics of the endothelium. *J Thromb Haemost* **3,** 1392–1406 (2005).
6. Aird, W. C. Endothelium in health and disease. *Pharmacol. Reports* **60,** 139–143 (2008).
7. Aird, W. C. Phenotypic heterogeneity of the endothelium: I. Structure, function, and mechanisms. *Circ. Res.* **100,** 158–173 (2007).
8. Levick, J. *An Introduction to Cardiovascular Physiology, Second Edition*. (Butterworth-Heinemann Ltd. Linacre House, Jordan Hill, Oxford OX2 8DP, 1995).
9. Burton, A. C. Relation of Structure of the Wall. *Physiol. Rev.* **34,** 619–642 (1954).
10. Alberts, B., Johnson, A., Lewis, J. & Al., E. *Molecular Biology of the Cell. 4th edition*. (New York: Garland Science, 2002).
11. Wang, J., Bingaman, S. & Huxley, V. H. Intrinsic sex-specific differences in microvascular endothelial cell phosphodiesterases. *Am. J. Physiol. Heart Circ. Physiol.* **298,** H1146-54 (2010).
12. Huxley, V. H., Wang, J. J. & Sarelius, I. H. Adaptation of coronary microvascular exchange in arterioles and venules to exercise training and a role for sex in determining permeability responses. *Am. J. Physiol. Heart Circ. Physiol.* **293,** H1196-205 (2007).
13. Huxley, V. H. & Wang, J. Cardiovascular sex differences influencing microvascular exchange. *Cardiovasc. Res.* **87,** 230–242 (2010).
14. Lorenz, M. *et al.* Does cellular sex matter? Dimorphic transcriptional differences between female and male endothelial cells. *Atherosclerosis* **240,** 61–72 (2015).
15. Addis, R. *et al.* Human umbilical endothelial cells (HUVECs) have a sex: characterisation of the phenotype of male and female cells. *Biol. Sex Differ.* **5,** 18 (2014).

16. Fadini, G. P. *et al.* Gender differences in endothelial progenitor cells and cardiovascular risk profile: The role of female estrogens. *Arterioscler. Thromb. Vasc. Biol.* **28,** 997–1004 (2008).

17. Whitley, H. P. & Lindsey, W. Sex-Based Differences in Drug Activity - American Family Physician. (2009).

18. Maas, A. H. E. M. & Appelman, Y. E. A. Gender differences in coronary heart disease. *Netherlands Hear. J.* **18,** 598–603 (2010).

19. Mathew J Reeves, P. *et al.* Sex differences in stroke: epidemiology, clinical presentation, medical care, and outcomes. *Lancet Naurol* **7,** 915–926 (2009).

20. Geary, G. G., Krause, D. N. & Duckles, S. P. Gonadal hormones affect diameter of male rat cerebral arteries through endothelium-dependent mechanisms. *Am. J. Physiol. Heart Circ. Physiol.* **279,** H610-8 (2000).

21. Fairweather, D., Frisancho-Kiss, S. & Rose, N. R. Sex differences in autoimmune disease from a pathological perspective. *Am. J. Pathol.* **173,** 600–9 (2008).

22. Ballotari, P., Venturelli, F., Greci, M., Giorgi Rossi, P. & Manicardi, V. Sex Differences in the Effect of Type 2 Diabetes on Major Cardiovascular Diseases: Results from a Population-Based Study in Italy. *Int. J. Endocrinol.* **2017,** 1–9 (2017).

23. Mehta, D. & Malik, A. B. Signaling Mechanisms Regulating Endothelial Permeability. *Physiol. Rev.* **86,** 279–367 (2006).

24. Komarova, Y. & Malik, A. B. Regulation of endothelial permeability via paracellular and transcellular transport pathways. *Annu. Rev. Physiol.* **72,** 463–93 (2010).

25. Curry, F. R. E. & Adamson, R. H. Vascular permeability modulation at the cell, microvessel, or whole organ level: Towards closing gaps in our knowledge. *Cardiovasc. Res.* **87,** 218–229 (2010).

26. Scallan, J., Huxley, V. H. & Korthuis, R. J. *Capillary Fluid Exchange: Regulation, Functions, and Pathology.* (San Rafael (CA): Morgan & Claypool Life Sciences, 2010).

27. Bagher, P. & Segal, S. S. The mouse cremaster muscle preparation for intravital imaging of the microcirculation. *J. Vis. Exp.* 2–7 (2011). doi:10.3791/2874

28. Leung, Y.-K., Mak, P., Hassan, S. & Ho, S.-M. Estrogen receptor (ER)-β isoforms: A key to understanding ER-β signaling. *Proc. Natl. Acad. Sci. U. S. A.* **103,** 13162–13167 (2006).

29. Nilsson, S. *et al.* Mechanisms of estrogen action. *Physiol. Rev.* **81,** 1535–65 (2001).

30. Evans, M. J., Harris, H. A., Miller, C. P., Karathanasis, S. K. & Adelman, S. J. Estrogen receptors alpha and beta have similar activities in multiple endothelial

cell pathways. *Endocrinology* **143,** 3785–95 (2002).

31. Toutain, C. E. *et al.* Estrogen receptor α expression in both endothelium and hematopoietic cells is required for the accelerative effect of estradiol on reendothelialization. *Arterioscler. Thromb. Vasc. Biol.* **29,** 1543–1550 (2009).

32. Holm, A., Andersson, K. E., Nordström, I., Hellstrand, P. & Nilsson, B.-O. Down-regulation of endothelial cell estrogen receptor expression by the inflammation promoter LPS. *Mol. Cell. Endocrinol.* **319,** 8–13 (2010).

33. Cid, M. C., Schnaper, H. W. & Kleinman, H. K. Estrogens and the vascular endothelium. *Ann. N. Y. Acad. Sci.* **966,** 143–57 (2002).

34. Huang, A., Sun, D., Koller, A. & Kaley, G. Gender difference in myogenic tone of rat arterioles is due to estrogen-induced, enhanced release of NO. *Am. J. Physiol.* **272,** H1804-9 (1997).

35. Brown, C. J. *et al.* Androgen receptor locus on the human X chromosome: regional localization to Xq11-12 and description of a DNA polymorphism. *Am. J. Hum. Genet.* **44,** 264–269 (1989).

36. Torres-Estay, V. *et al.* Androgen receptor in human endothelial cells. *J. Endocrinol.* **224,** R131–R137 (2015).

37. Nheu, L. *et al.* Physiological effects of androgens on human vascular endothelial and smooth muscle cells in culture. *Steroids* **76,** 1590–6 (2011).

38. Sieveking, D. P. *et al.* A sex-specific role for androgens in angiogenesis. *J. Exp. Med.* **207,** 345–352 (2010).

39. Castela, A., Vendeira, P. & Costa, C. Testosterone, endothelial health, and erectile function. *ISRN Endocrinol.* **2011,** 1–7 (2011).

40. Lu, Y. L. *et al.* Changes in aortic endothelium ultrastructure in male rats following castration, replacement with testosterone and administration of 5α-reductase inhibitor. *Asian J. Androl.* **9,** 843–847 (2007).

41. Bazzoni, G. & Dejana, E. Endothelial cell-to-cell junctions: molecular organization and role in vascular homeostasis. *Physiol Rev.* **84,** 869–901 (2004).

42. Giannotta, M., Trani, M. & Dejana, E. VE-cadherin and endothelial adherens junctions: Active guardians of vascular integrity. *Dev. Cell* **26,** 441–454 (2013).

43. Angst, B. D., Marcozzi, C. & Magee, A. I. The cadherin superfamily: diversity in form and function. *J. Cell Sci.* **114,** 629–641 (2001).

44. Gory-Fauré, S. *et al.* Role of vascular endothelial-cadherin in vascular morphogenesis. *Development* **126,** 2093–2102 (1999).

45. Wu, Y., Stabach, P., Michaud, M. & Madri, J. A. Neutrophils Lacking Platelet-Endothelial Cell Adhesion Molecule-1 Exhibit Loss of Directionality and Motility in CXCR2-Mediated Chemotaxis. *J. Immunol.* **175,** 3484–3491 (2005).

46. Woodfin, A., Voisin, M. B. & Nourshargh, S. PECAM-1: A multi-functional molecule in inflammation and vascular biology. *Arterioscler. Thromb. Vasc. Biol.* **27,** 2514–2523 (2007).

47. Graesser, D. *et al.* Altered vascular permeability and early onset of experimental autoimmune encephalomyelitis in PECAM-1-deficient mice. *J. Clin. Invest.* **109,** 383–392 (2002).

48. Delisser, H. *et al.* Involvement of Endothelia PECAM-1/CD31 in Angiogenesis. *Am. J. phatology* **151,** 671–677 (1997).

49. Granger, D. & Senchenkova, E. *Inflammation and the Microcirculation.* (San Rafael (CA): Morgan & Claypool Life Sciences, 2010).

50. Lawson, C. & Wolf, S. ICAM-1 signaling in endothelial cells. *Pharmacol Rep* **61,** 22–32 (2009).

51. Sumagin, R. & Sarelius, I. H. TNF-α ACTIVATION OF ARTERIOLES AND VENULES ALTERS THE DISTRIBUTION AND LEVELS OF ICAM-1 AND AFFECTS LEUKOCYTE-ENDOTHELIAL CELL INTERACTIONS. *Am. J. Physiol. Heart Circ. Physiol.* **291,** 1–23 (2006).

52. Sumagin, R., Lomakina, E. & Sarelius, I. H. Leukocyte-endothelial cell interactions are linked to vascular permeability via ICAM-1-mediated signaling. *Am. J. Physiol. - Hear. Circ. Physiol.* **295,** H969–H977 (2008).

53. Sumagin, R., Kuebel, J. M. & Sarelius, I. H. Leukocyte rolling and adhesion both contribute to regulation of microvascular permeability to albumin via ligation of ICAM-1. *Am. J. Physiol. - Cell Physiol.* **301,** C804–C813 (2011).

54. Cybulsky, M. I. *et al.* A major role for VCAM-1, but not ICAM-1, in early atherosclerosis. *J. Clin. Invest.* **107,** 1255–1262 (2001).

55. Deem, T. L. & Cook-mills, J. M. Vascular cell adhesion molecule 1 (VCAM-1) activation of endothelial cell matrix metalloproteinases : role of reactive oxygen species. **104,** 2385–2394 (2016).

56. Hackman, A. *et al.* Levels of Soluble Cell Adhesion Molecules in Patients With Dyslipidemia. *Circulation* **93,** 1334 LP-1338 (1996).

57. Videm, V. & Albrigtsen, M. Soluble ICAM-1 and VCAM-1 as markers of endothelial activation. *Scand. J. Immunol.* **67,** 523–531 (2008).

58. Navarro, P., Ruco, L. & Dejana, E. Differential localization of VE- and N-cadherins in human endothelial cells: VE-cadherin competes with N-cadherin for junctional localization. *J. Cell Biol.* **140,** 1475–1484 (1998).

59. Gerhardt, H., Wolburg, H. & Redies, C. N-cadherin mediates pericytic-endothelial interaction during brain angiogenesis in the chicken. *Dev. Dyn.* **218,** 472–9 (2000).

60. Tillet, E. *et al.* N-cadherin deficiency impairs pericyte recruitment, and not endothelial differentiation or sprouting, in embryonic stem cell-derived

angiogenesis. *Exp. Cell Res.* **310,** 392–400 (2005).

61. Luo, Y. & Radice, G. L. N-cadherin acts upstream of VE-cadherin in controlling vascular morphogenesis. *J. Cell Biol.* **169,** 29–34 (2005).

62. Ning, L. *et al.* Interactions between ICAM-5 and β1 integrins regulate neuronal synapse formation. *J. Cell Sci.* **126,** 77–89 (2013).

63. Short, S. M., Talbott, G. A. & Juliano, R. L. Integrin-mediated signaling events in endothelial cells. *Mol. Biol. Cell* **9,** 1969 (1998).

64. Dejana, E., Zanetti, A., Dominguez-Jimenez, C. & Conforti, G. in *Angiogenesis in Health and Disease* (eds. Maragoudakis, M. E., Gullino, P. & Lelkes, P. I.) 91–98 (Springer US, 1992). doi:10.1007/978-1-4615-3358-0_8

65. Danhier, F., Le Breton, A. & Préat, V. RGD-based strategies to target alpha(v) beta(3) integrin in cancer therapy and diagnosis. *Mol. Pharm.* **9,** 2961–73 (2012).

66. Horton, M. A. The αvβ3 integrin 'vitronectin receptor'. *Int. J. Biochem. Cell Biol.* **29,** 721–725 (1997).

67. Abràmoff, M. D., Magalhães, P. J. & Ram, S. J. Image processing with imageJ. *Biophotonics Int.* **11,** 36–41 (2004).

68. Flow Cytometry Basics Guide. *Bio-Rad Lab. Inc.* 1–68 (2003).

69. Higgins, J. J. *Introduction to Modern Nonparametric Statistics*. (Brookes/Cole, Cengage Learning, 2004).

70. Johnson, M. Statistics and Data Analysis Individual Growth Analysis Using PROC MIXED Maribeth Johnson , Medical College of Georgia , Augusta , GA. *Analysis* 1–7 (1998).

71. Gavard, J. Endothelial permeability and-VE cadherin: A wacky comradeship. *Cell Adhes. Migr.* **8,** 158–164 (2014).

72. Carmeliet, P. *et al.* Targeted Deficiency or Cytosolic Truncation of the VE-cadherin Gene in Mice Impairs VEGF-Mediated Endothelial Survival and Angiogenesis. *Cell* **98,** 147–157 (1999).

73. Zanetta, L. *et al.* Expression of Von Willebrand factor, an endothelial cell marker, is up-regulated by angiogenesis factors: a potential method for objective assessment of tumor angiogenesis. *Int J Cancer.* **85,** 281–288 (2000).

74. Schlingemann, R. O. *et al.* Differential expression of markers for endothelial cells, pericytes, and basal lamina in the microvasculature of tumors and granulation tissue. *Am. J. Pathol.* **138,** 1335–1347 (1991).

75. Voyta, J. C., Via, D. P., Butterfield, C. E. & Zetter, B. R. Identification and isolation of endothelial cells based on their increased uptake of acetylated low density lipoprotein. *J. Cell. Biol.* **99,** 2034–2040 (1994).

76. Li, X.-M., Hu, Z., Jorgenson, M. L. & Slayton, W. B. High levels of acetylated

low density lipoprotein uptake and low Tie2 promoter activity distinguishes sinusoids from other vessel types in the murine bone marrow. *Circulation* **120,** 1–18 (2009).

77. Laitinen, L. Griffonia simplicifolia lectins bind specifically to endothelial cells and some epithelial cells in mouse tissues. *Histochem. J.* **19,** 225–234 (1987).

78. Sahagun, G., Moore, S. a, Fabry, Z., Schelper, R. L. & Hart, M. N. Purification of murine endothelial cell cultures by flow cytometry using fluorescein-labeled griffonia simplicifolia agglutinin. *Am. J. Pathol.* **134,** 1227–1232 (1989).

79. DeCicco-Skinner, K. L. *et al.* Endothelial cell tube formation assay for the in vitro study of angiogenesis. *J. Vis. Exp.* **10,** e51312 (2014).

80. Berta, P. *et al.* Genetic evidence equating SRY and the testis-determining factor. *Nature* **348,** 448–450 (1990).

81. An, J., Beauchemin, N., Albanese, J. & Sullivan, A. K. Use of a Rat cDNA Probe Specific for the Y Chromosome to Detect Male-Derived Cells. *Journa* **18,** 289–293 (1997).

82. Claesson-Welsh, L. Vascular permeability—the essentials. *Ups. J. Med. Sci.* **120,** 135–143 (2015).

83. Casimir, G. J. A. & Duchateau, J. Gender differences in inflammatory processes could explain poorer prognosis for males. *J. Clin. Microbiol.* **49,** 478 (2011).

84. Janssen, I., Heymsfield, S. B., Wang, Z. & Ross, R. Skeletal muscle mass and distribution in 468 men and women aged 18–88 yr. *J. Appl. Physiol.* **89,** 81 LP-88 (2000).

85. Huxley, V. & Rumbaut, R. The Microvasculature As A Dynamic Regulator Of Volume And Solute Exchange. *Clin. Exp. Pharmacol. Physiol.* **27,** 847–854 (2000).